Impact of the N-terminal secretor domain on YopD translocator function in *Yersinia pseudotuberculosis* type III secretion

Ayad A. A. Amer,[1,2] Monika K. Åhlund,[1,4] Jeanette E. Bröms,[3,5] Åke Forsberg[1,2,3] and Matthew S. Francis[1,2,#]

Department of Molecular Biology[1] and Umeå Center for Microbial Research,[2] Umeå University, SE-901 87 Umeå, and Department of Medical Countermeasures, Swedish Defense Research Agency, Division of NBC-Defense, SE-901 82 Umeå,[3] Sweden

Running head: YopD N-terminal secretion signal

[#] Corresponding author: Mailing address: Department of Molecular Biology, Umeå University, SE-901 87 Umeå, Sweden. Phone: +46-(0)90-7856752. Fax: +46-(0)90-772630. Email: matthew.francis@molbiol.umu.se

[4] Present address: Department of Medical Biochemistry and Biophysics, Umeå University, SE-901 87 Umeå, Sweden

[5] Present address: Department of Clinical Bacteriology, Umeå University, SE-901 85 Umeå, Sweden

Type III secretion systems (T3SSs) secrete needle components, pore-forming translocators and the translocated effectors. In part, effector recognition by a T3SS involves their N-terminal amino acids and their 5´ mRNA. To investigate if similar molecular constraints influence translocator secretion we scrutinized this region within YopD from *Yersinia pseudotuberculosis.* Mutations in the 5´ end of *yopD* that resulted in specific disruption of the mRNA sequence did not affect YopD secretion. On the other hand, a few mutations affecting the protein sequence reduced secretion. Translational reporter fusions identified the first five codons as a minimal N-terminal secretion signal and also indicated that the YopD N-terminus might be important for *yopD* translation control. Hybrid proteins in which the N-terminus of YopD was exchanged with the equivalent region of the YopE effector or the YopB translocator were also constructed. While the *in vitro* secretion profile was unaltered, these modified bacteria were all compromised in T3SS activity in the presence of immune cells. Thus, the YopD N-terminus does harbor a secretion signal that may also incorporate mechanisms of *yopD* translation control. This signal tolerates a high degree of variation while still maintaining secretion competence suggestive of inherent structural peculiarities that make it distinct from secretion signals of other T3SS substrates.

A wide variety of Gram negative bacteria utilize type III secretion systems to encounter diverse hosts such as humans, animals, plants, fish and insects (58, 76). Inherent in this host interaction strategy is a multi-component protein assembly spanning the bacterial envelope that is coupled to an extracellular protruding needle-like appendage. When in contact with eukaryotic cells, this injection device has the capacity to translocate an extensive array of protein cargo from the bacterial cytoplasm and/or the bacterial surface directly into the target cell interior (3, 63). Internalized bacterial proteins dismantle the inner processes of the host cell, creating a more hospitable environment for bacterial survival and colonization. Laboratory grown bacteria can also use their T3SS to secrete proteins into the extracellular milieu (31).

In general, three types of protein substrate are secreted by a T3SS; components of the external needle, the translocated effectors and the translocator proteins (58, 76). These latter proteins are essential for the translocation process by forming at the needle tip, a pore-like translocon in the eukaryotic cell plasma membrane (53). These pores may therefore complete an uninterrupted type III secretion (T3S) channel that links the bacterial interior to that of the eukaryotic cell. Although direct experimental evidence is lacking, effectors could pass through this translocon conduit to localize inside the eukaryotic cell.

Multiple T3S signals are evident for effector substrates. Most effectors require small molecular weight chaperones for their stability and/or efficient secretion (26). Some of these chaperones are known to interact with the T3S ATPase energizer at the cytoplasmic base of the T3SS (2, 32). A chaperone-independent secretion signal also exists at the extreme N-terminus, represented by a complex combination of the mRNA as well as protein sequence (16, 46, 69). While no sequence consensus is visually obvious, there is some evidence of an amphipathic property (47) and various computational approaches based upon sophisticated machine-learning methodology can predict T3S substrates on the basis of a conserved secretion signal (6, 48, 64, 84). Nevertheless, what molecular contribution these extensively mapped chaperone-independent signals impart in substrate secretion is not yet understood. However, it must be universally recognized considering T3SSs are promiscuous often allowing the secretion of non-native substrates.

N-terminal secretion signals of the translocator proteins are considerably less defined. Perhaps this putative secretion signal is unique, allowing the T3SS to distinguish translocator and effector cargo (67). A secretion signal of SipB from *Salmonella enterica* Typhimurium lies between residues 3 and 8 of the N-terminus (41). Polar residues in the extreme N-terminus contributed to the secretion of IpaC by *Shigella flexneri* (35). Moreover, secretion of LcrV by *Yersinia* requires information between residues 2 to 4 and 11

to 13 (12). At least these data do indicate the existence of an N-terminal chaperone-independent signal for the translocators, reminiscent of the well-studied effector N-terminal secretion signal. Furthermore, these respective signals are interchangeable without apparent loss of biological function (54).

This study looked to extend our knowledge of the translocator N-terminus by investigating what role this domain played in the activity of the YopD translocator from *Y. pseudotuberculosis.* This 306 amino acid protein possesses multiple functions critical for *Yersinia* Ysc-Yop T3S. In the *Yersinia* cytoplasm, YopD stability depends on an interaction with its customized T3S chaperone, LcrH (20, 27, 79). YopD-LcrH complexes cooperates with the LcrQ regulatory element to bind the 5' untranslated regions (UTRs) of *yop* mRNA and impose post-transcriptional silencing of Yop synthesis by either blocking translation and/or promoting degradation of mRNA (4, 13). Upon secretion, YopD forms pores in the infected cell plasma membrane through which the effectors might gain access into the host cell interior (34, 55, 57, 72). This extracellular function depends on self-assembly and additional interactions with LcrV and YopB (17). Thus, a Δ*yopD* null mutant is de-regulated for Yops synthesis and although Yops secretion functions normally, Yops delivery into cells is completely abolished (29, 36, 62, 81). Despite this knowledge of YopD function, information about the chaperone-dependent and –independent signals actually needed for YopD secretion are still lacking. To amend this, a series of N-terminal substitution and deletion mutations, as well as translational reporter fusions, were used to investigate the N-terminal signal for YopD secretion. Our data suggests as few as five N-terminal residues are sufficient for T3S of YopD. Of importance among these are the isoleucines at positions 3 and 5, or their corresponding codons ‘ATA’ and ‘ATC’. Only a few of the many mutations actually impinged on YopD secretion, suggesting that the molecular framework of the YopD N-terminal secretion signal is extremely robust and capable of tolerating a remarkable degree of physio-chemical alteration. Effector translocation was seldom compromised, also suggesting that the N-terminus is not required for the extracellular function of YopD. Interestingly, YopD synthesis was diminished in some key variants, indicating a possible role for some aspect of the 5′ end of *yopD* in translation control. Moreover, domain swapping experiments involving the N-terminal secretion signals of YopD and the YopE effector molecule compromised T3SS activity. This may indicate that the N-terminal secretion signal has evolved specifically for and function best for only their substrate ensuring timely delivery and/or function of Yops during intimate bacteria-host cell contact.

MATERIALS AND METHODS

Bacterial strains and growth conditions. Strains used in this study are listed in Table 1. Routine bacterial culturing of *E. coli* and *Y. pseudotuberculosis* was performed at 37°C and 26°C respectively, typically in Luria Bertani (LB) broth. When examining protein expression and secretion from *Yersinia*, strains were grown in brain heart infusion (BHI) broth, both in minus calcium (BHI supplemented with 5mM EGTA, 20mM $MgCl_2$ – T3S permissive medium) and in plus calcium (2.5mM $CaCl_2$ – T3S non-permissive medium) conditions. In both cases, bacteria were grown in the presence of 0.025% (v/v) Triton X-100. This treatment detached Yops prone to associate to the bacterial surface (3), thereby ensuring that our T3S analysis would include all Yops secreted beyond the bacterial envelope. When appropriate, antibiotics at the following concentrations were used to select for plasmid maintenance during culturing: Carbenicillin (Cb) 100µg/ml, Chloramphenicol (Cm) 25µg/ml, and Kanamycin (Km) 50µg/ml. These plasmids are listed in Supplementary Table S1 (available for download online).

Mutant construction. N-terminal YopD variants were created by the overlap PCR method using the various primer pairs listed in Supplementary Table S2. PCR fragments were cloned directly into pCR®4-TOPO® (Invitrogen) and each mutation confirmed by sequence analysis (Eurofins MWG Operon, Ebersberg, Germany). Confirmed DNA fragments were then lifted into the pDM4 suicide mutagenesis vector (52) following XhoI-XbaI restriction. *E. coli* S17-1λpir harboring the different mutagenesis constructs were used as donor strains in conjugations with *Y. pseudotuberculosis*. Appropriate allelic exchange events were monitored by Cm sensitivity and sucrose resistance. All mutants were confirmed by a combination of PCR and sequence analysis.

Exchange of the YopD N-terminal region with the equivalent sequence from the YopE effector substrate was also performed by overlap PCR with the primer combinations listed in Supplementary Table S2. Unless otherwise stated, the region exchanged encompassed residues 2 to 15. Significantly, each chimeric variant was again introduced *in cis* on the *Y. pseudotuberculosis* virulence plasmid to ensure expression occurred in the context of native regulatory elements.

mRNA structural predictions. Sequences at the 5´termini of various *yopD* alleles, including 45 nucleotides (nt) upstream and 57 nt downstream of the AUG start codon, were predicted using the RNA

Mfold version 3.2 software (87) available online at http://mfold.bioinfo.rpi.edu/cgi-bin/rna-form1.cgi. Structures were defined with default settings.

Transcriptional analysis by semi-quantitative reverse transcription-PCR. The isolation of total RNA from *Yersinia*, the reverse transcription of this mRNA into cDNA and its use as template for subsequent PCR amplification with the gene specific primers listed in Supplementary Table S2 is described in detail elsewhere (14).

Analysis of Yop synthesis and secretion. Yop synthesis and secretion by *Y. pseudotuberculosis* was analyzed after log-phase growth in permissive (without Ca^{2+}) and non-permissive (with Ca^{2+}) fresh BHI media for 1 hr at 26°C and, following the addition of 0.025% (v/v) Triton X-100, a further 3 hrs at 37°C. Measurements at OD_{600} were used to standardize each culture. Samples of these suspensions were then taken to represent the total protein fraction. Bacteria were then collected by a 2 min centrifugation from which samples of the cleared bacterial supernatant were gathered (represents secreted Yops fraction). All samples were added to 4x SDS-PAGE loading buffer (200mM Tris-HCl, pH 6.8, 8% SDS, 0.4% Bromophenol blue, 40% Glycerol, 20% β-Mercaptoethanol), denatured and then fractionated by 12% sodium dodecyl sulfate-polyacrylamide gel electrophoresis (SDS-PAGE) and western blot using rabbit α-YopD, α-YopB, α-LcrV and α-YopE polyclonal antisera (Agrisera, Vännäs, Sweden) in combination with α-rabbit antiserum conjugated with horse radish peroxidase (GE Healthcare, Buckinghamshire, United Kingdom). Homemade chemiluminescent solutions were used to detect individual protein bands. Quantification by western blotting mirrored previously published methods (8) and used the Quantity One software, version 4.52 (Bio-Rad).

Intracytoplasmic YopD stability assay. To assess the stability of pre-made YopD built up in the bacterial cytoplasm, we employed the intrabacterial stability assay of Feldman and colleagues (24) using either chloramphenicol or tetracycline as the *de novo* protein synthesis inhibitor. Note that this steady-state experiment is designed to measure the steady-state stability of accumulated YopD or YopD-Bla variants and not the efficiency of *de novo* translation.

Low calcium growth measurements. Determination of the *Yersinia* low calcium response growth phenotypes when grown under high- and low-Ca^{2+} conditions at 37°C were performed by measuring absorbance at 600nm during growth in liquid Thoroughly Modified Higuchi's (TMH) medium (minus Ca^{2+}) or TMH medium supplemented with 2.5 mM $CaCl_2$ (plus Ca^{2+}) (17). Parental *Yersinia* (YPIII/pIB102) are defined as calcium dependent (CD), since they are unable to grow in the absence of Ca^{2+} at 37°C, while

Yersinia lacking the *lcrQ* allele, such as the Δ*yscU,* Δ*lcrQ* mutant (YPIII/pIB75-26) is termed temperature sensitive (TS) reflecting its inability to grow at 37°C.

Cytotoxicity assay. Cultivation and infection of HeLa cells for cytotoxicity assays was performed on cover slips and using our standard methods (29, 62). At numerous intervals post-infection, culture medium was replaced by 2% paraformaldehyde fixation solution and then mounted on glass slides. The extent of morphological change was visualized by phase contrast microscopy using a Nikon Eclipse 90i microscope. Cytotoxicity resulting from infection with parental *Y. pseudotuberculosis* (YPIII/pIB102) defined the upper limit, while the lower limit was defined by a Δ*yopD* deletion mutant YPIII/pIB625 ($YopD_{\Delta 4\text{-}20}$) (57).

Bacterial viability in the presence of eukaryotic cells. Essentially, the method of Bartra and co-workers (7) was used to establish bacterial viability in the presence of murine macrophage-like J774 cells. In essence, bacteria lacking a fully functional T3SS are more readily phagocytosed and are therefore more susceptible to the antimicrobial effects of J774 cells. This reduced viability was determined by performing colony forming unit (CFU) counts for relevant bacterial strains in infected eukaryotic cell lysates.

Construction and analysis of YopD translationally fused to signalless β-Lactamase. A 5-prime truncated *bla* gene was amplified with the primer pair listed in Supplementary Table S1 using pAJR104 as template DNA. This Kpn-EcoRI DNA fragment was cloned into pMMB208, thereby placing the *bla* reporter under IPTG inducible control. Various length translational fusions linking the 5-prime region of *yopD,* including the predicted Shine-Dalgarno (SD) sequence, to truncated *bla* were then generated in this background. This was achieved by a BamHI-KpnI cloning in two ways. Larger DNA fragments (> 75 base pairs) were first amplified by PCR with the appropriate primer pairings listed in Supplementary Table S2 and using lysed YPIII/pIB102 as a source of template DNA. Smaller DNA fragments (< 45 base pairs) were formed by the annealing of two complementary oligonucleotides prior to DNA ligation to the vector (Supplementary Table S2). Analysis of recombinant β-Lactamase synthesis and secretion followed the procedure for Yop synthesis and secretion. After western blot of fractionated protein, fusion proteins were detected with a primary rabbit polyclonal anti-β-Lac antibody (Millipore AB, Solna, Sweden) followed by incubation with α-rabbit antiserum conjugated with horse radish peroxidase (GE Healthcare). Relative western blot signal intensities were quantified by an established protocol (8) using Quantity One software, version 4.52 (Bio-Rad).

Statistics. The values are expressed as mean ± standard error (mean ± SE) of multiple independent experiments. The non-parametric Mann-Whitney *U* test was used to analyze the differences in 1) percent Yop secretion efficiency when compared to native Yop secretion, 2) Yop-Bla secretion efficiency when compared to YopD20-Bla and 3) relative viability determined by the ratio of CFU/ml between mutant bacteria (producing the chimeras) and bacteria producing $YopD_{high(x2)}$, which was phenotypically indistinguishable from parental bacteria. Differences were considered significant with a probability value of $p < 0.05$ (two-tailed).

RESULTS

YopD secretion is affected by an N-terminal frame shift mutation. A T3S signal sequence is located in the N-terminus of various effector proteins (16, 46, 69). It probably comprises a combination of the 5-prime mRNA sequence and the amino acid sequence. A similar combination of signals may also exist for the translocator proteins, but this has not been conclusively demonstrated (12, 35, 41, 54). YopD, a translocator protein functioning as a component of the Ysc-Yop T3SS of *Yersinia*, possesses an N-terminal domain necessary for efficient secretion (57). To dissect how this region contributes to YopD secretion, a series of *in cis* mutations were generated in the *yopD* allele. This enabled production under normal regulatory control of YopD variants with alterations to the first 15 residues of their N-terminus. The first mutant ($YopD_{Frame+1}$) harbors a +1 frame shift, in which the nucleotide `A´ was inserted immediately after the start codon of YopD and then compensated by the removal of a `T´ at position 46 to restore the reading frame after codon 15 (Table 2). The second mutant ($YopD_{Frame-1}$) was a −1 frameshift. Since a deletion of the first nucleotide after the start codon would result in a premature stop codon, the ninth nucleotide (an `A´) was removed and at position 46 a `T´ was inserted to again restore the reading frame after codon 15 (Table 2). These mutants were designed to assess if the secretion signal is protein-based; both constructs carry altered amino acid sequences, but the mRNA sequences closely resemble that of native YopD ($YopD_{wild\ type}$). Another mutant ($YopD_{Scramble}$) was constructed by mutating all possible nucleotides in the wobble position of each codon in the YopD N-terminus, while still maintaining a wild type amino acid sequence. This resulted in a YopD variant with a scrambled 5´ mRNA coding sequence designed to gauge the contribution of mRNA to YopD secretion. In fact, 16 nt substitutions of a possible 45 were generated (Table 2). Importantly, none of the

mutations impacted on the stability of accumulated cytoplasmic-located YopD, since all variants were as resistant to intrabacterial proteases as was $YopD_{wild\ type}$ (Fig. 1).

Yop synthesis and secretion was next examined by growing bacteria in either Yop-inducing (minus Ca^{2+}) or non-inducing (plus Ca^{2+}) BHI broth. The extent of mutated YopD associated with bacteria did not deviate from that observed for parental bacteria (Fig. 2A, upper panel). This was confirmed by quantifying the total $YopD_{Frame+1}$ (92.9%), $YopD_{Frame-1}$ (93.3%) and $YopD_{Scramble}$ ()5.3%) synthesis relative to native YopD (Fig. 2B). It indicated that the well-established Ca^{2+}-dependent regulation of Yop synthesis is not affected by these alterations to the YopD N-terminus. In contrast, a marked reduction of $YopD_{Frame+1}$, but not $YopD_{Frame-1}$ or $YopD_{Scramble}$, was evident in the supernatant fraction of these bacteria when grown in Yop-inducing media (Fig. 2A, lower panel). In fact, this equated to only 25.2% of synthesized $YopD_{Frame+1}$ that was actually secreted (Fig 2B, light gray box). Moreover, the efficiency of $YopD_{Frame+1}$ secretion was significantly reduced to 29.3% of native YopD (Fig. 2B, dark gray box, p=0.0079, **). This poor $YopD_{Frame+1}$ secretion efficiency was not caused by a general secretion defect because the slight affect on the secretion of other Yops such as YopE (73.4% secretion efficiency) was not statistically significant (Fig. 2B, dark gray box, p=0.1143). Finally, secretion was dependent on the Ysc-Yop T3SS because mutant bacteria lacking the *yscU* and *lcrQ* alleles did not secrete any Yops (Fig. 2A and data not shown). We therefore conclude that $YopD_{Frame+1}$ possesses an intrinsic T3S defect.

These data primarily suggest an involvement of the amino acid sequence in ensuring efficient YopD secretion. However, they do not necessarily rule out a role for mRNA. We were therefore curious to model the predicted mRNA secondary structure of these *yopD* alleles, focusing on sequence encompassing the AUG start codon and 45 nt upstream and 57 nt downstream. This modeling revealed very similar mRNA structures for $YopD_{wild\ type}$ (Supplementary Fig. S1A), $YopD_{Frame+1}$ (Fig. S1B) and $YopD_{Frame-1}$ (Fig. S1C), whereas the $YopD_{Scramble}$ mRNA structure was considerably different (Fig. S1D). Given that $YopD_{Frame+1}$ is the only variant poorly secreted, it is therefore hard to envision how these mRNA structures could constitute a secretion signal *per se*.

N-terminal isoleucines contribute to YopD secretion. In light of the defect in $YopD_{Frame+1}$ secretion, it is curious as to why the secretion of $YopD_{Frame-1}$ was unaffected. We tested the possibility that the remaining wild type polar threonine and isoleucine residues at positions 2 and 3 respectively (Table 2) were adequate to promote secretion of this variant. However, individual substitution mutations replacing these two residues

with amino acids of varying physical properties (Glycine, Asparagine and Lysine) in both $YopD_{wild\ type}$ and $YopD_{Frame-1}$ backgrounds had no effect on Yops synthesis or secretion (Supplementary Fig. S2). Nevertheless, an additional isoleucine residue is also located at position 4 in $YopD_{Frame-1}$ and position 5 in native YopD (Table 2). Since a few studies have pointed towards isoleucine being a vital aspect of T3S targeting of some Yops (59, 60), we generated two double mutants exchanging both isoleucines for asparagine, giving rise to $YopD_{I3,5N}$ and $YopD_{Frame-1,\ I3,4N}$. Intracellular pools of both mutants were stable (Fig. 1) and permitted generous synthesis of all Yops during bacterial growth in inducing conditions (Fig. 3A, upper panel and data not shown), although the I3,5N mutation did alter the migration of YopD on SDS-PAGE. More interesting however was that this $YopD_{I3,5N}$ variant secreted just 51.4% of synthesized protein, while the $YopD_{Frame-1,\ I3,5N}$ variant secreted 75.6% (Fig. 3A, lower panel and Fig. 3B, light gray box). Compared to native YopD, this represented a significant reduction in $YopD_{I3,5N}$ secretion efficiency of 55.5% (Fig. 3B, dark gray box, p=0.0079, **). However, the calculated $YopD_{Frame-1,\ I3,5N}$ secretion efficiency of 79.8% was not considered to be statistically different (p=0.1508). Crucially, this secretion defect was not observed for any other Yop including YopE (Fig. 3A, lower panel, Fig. 3B and data not shown). *In silico* mRNA secondary structure predictions cannot easily reconcile these differences because the generated models of $YopD_{I3,5N}$ (Supplementary Fig. S1E), $YopD_{Frame-1,\ I3,4N}$ (Fig. S1F) and $YopD_{wild\ type}$ (Fig. S1A) mRNA all appear appreciably different from each other. Hence, these data do not explain why $YopD_{Frame-1}$ is still efficiently secreted. Never the less, they do highlight a combined contribution of the N-terminal residues Ile-3 and Ile-5 to the secretion of native YopD.

YopD secretion is supported by an artificial amphipathic N-terminal signal sequence. A recent molecular analysis of T3S signals was performed by replacing amino acids 2 to 8 of the secreted protein YopE with all combinations of synthetic serine and isoleucine sequences (47). This revealed that amphipathic N-terminal sequences containing four or five serine/isoleucine residues are more likely to target YopE for secretion than stretches of hydrophobic or hydrophilic sequences. We therefore wondered whether amphipathicity is also a feature of the N-terminal YopD secretion signal. This was investigated by appending artificial sequences to the YopD N-terminus that efficiently secreted (NH_3-Ile-Ile-Ser-Ser-Ile-Ser-Ser-CO_2) (designated as 'high') or abolished (NH_3-Ile-Ile-Ile-Ile-Ser-Ile-Ile-CO_2) ('low') YopE secretion (47). These sequences were first used in single copy to replace amino acids 2 to 8 of YopD ($YopD_{high}$ and $YopD_{low}$)

(Table 2). Once again, to avoid any copy number effects, these constructs were placed *in cis* on the virulence plasmid. In contrast to the YopE study (47), no difference in synthesis or secretion could be observed for either $YopD_{high}$ or $YopD_{low}$ (Fig. 4). Thus, T3S of YopD is supported by an artificial secretion signal appended to the N-terminus. Moreover, while the two studies were performed differently – YopE was produced *in trans,* while YopD *in cis* – the fact that $YopD_{low}$ was still secreted could also imply that native secretion signals of both middle (translocator) and late (effector) substrates may differ with respect to the degree of amphipathicity required for their respective secretion.

We attempted to address this aspect further by creating another two constructs, $YopD_{high(x2)}$ and $YopD_{low(x2)}$. In these variants, the respective 'high' and 'low' synthetic sequences were duplicated thereby replacing codons 2 to 15 of native YopD (Table 2). We hypothesized that these two constructs would represent the maximal extremes in possible amphipathic tendencies at the YopD N-terminus. $YopD_{high(x2)}$ synthesis and secretion (Fig. 4) and the stability of pre-made pools accumulated in the cytoplasm (Fig. 1) still occurred in a manner reminiscent of $YopD_{wild\ type}$. In contrast, production of $YopD_{low(x2)}$ was surprisingly very low in our assay conditions (Fig. 4). To investigate the basis for this phenotype, we first isolated mRNA and reverse transcribed this into cDNA. Using this cDNA as template in PCR with *yopD* gene specific primers, no differences in Ca^{2+}-dependent transcription from the various mutated *yopD* alleles was observed (Fig. 5). In fact, this *yopD* transcription pattern mirrored the Ca^{2+}-dependent expression of the *yopE* gene encoding a late Ysc-Yop T3SS effector substrate (Fig. 5). We also examined the regulatory phenotype of this $YopD_{low(x2)}$ mutant using the dual approach of a low calcium response growth assay in parallel with a more thorough analysis of type III substrate synthesis and secretion. When grown at 37°C, parental bacteria typically displayed a strict CD growth phenotype (Fig. 6A), which was mirrored by strains producing the variants $YopD_{high}$ (Fig. 6B), $YopD_{low}$ (Fig. 6C) and $YopD_{high(x2)}$ (Fig. 6D). The Δ*yscU, lcrQ* double mutant exhibited a characteristic TS growth phenotype irrespective of Ca^{2+} concentration (Fig. 6F). However, bacteria producing $YopD_{low(x2)}$ were intermediate in their CD growth (Fig. 6E), a phenotype we have previously referred to as CD-like (17). Consistent with this subtle alteration in low calcium responsiveness, mutant bacteria producing $YopD_{low(x2)}$ were also modestly relaxed for calcium-dependent control of Yop synthesis. Production of YopB and LcrV was more abundant during conditions non-permissive for T3S, where LcrV was also secreted (Fig. 4). Collectively, these are all key indicators of compromised *yop*-regulatory control in *Yersinia* (17, 28, 57, 66, 81), suggesting that $YopD_{low(x2)}$-producing bacteria are subtly

de-regulated for Yops synthesis. Curiously, this modest regulatory defect was not evident at the transcriptional level. In this case, *yop* transcription was restricted to T3S-permissive growth conditions (Fig. 5). This prompted us to compare the secondary structure of 5´- mRNA derived from *yopD* alleles producing $YopD_{high(x2)}$ and $YopD_{low(x2)}$. Interestingly, the AUG start codon of mRNA encoding $YopD_{low(x2)}$ is potentially buried in an extended stem-loop structure (compare Supplementary Fig. S1H with S1G), which could conceivably alter translational control. Even if rate of translation is unperturbed, low $YopD_{low(x2)}$ amounts could be partly explained by an observed decrease in intracytoplasmic stability. Oddly, of all the YopD mutants constructed, accumulated pre-made pools of $YopD_{low(x2)}$ was notably more sensitive to endogenous protease digestion (Fig. 1). Why this particular genetic exchange results in a YopD variant with elevated steady-state instability is not yet understood. Collectively though, these unexpected observations curtailed any further investigation into the role of N-terminal sequence amphipathicity in YopD secretion. However, $YopD_{low(x2)}$ might prove a useful tool in investigating unknown mechanisms of translational control of YopD.

YopD secretion is affected by N-terminal deletions. To further dissect the YopD N-terminus, we created a series of 13 progressively smaller *in cis* deletion mutations between codons 4 and 20. These mutated alleles encoded the variants $YopD_{\Delta 5\text{-}19}$, $YopD_{\Delta 6\text{-}19}$, $YopD_{\Delta 7\text{-}19}$, $YopD_{\Delta 8\text{-}19}$, $YopD_{\Delta 9\text{-}19}$, $YopD_{\Delta 10\text{-}19}$, $YopD_{\Delta 11\text{-}19}$, $YopD_{\Delta 12\text{-}19}$, $YopD_{\Delta 13\text{-}19}$, $YopD_{\Delta 14\text{-}19}$, $YopD_{\Delta 15\text{-}19}$, $YopD_{\Delta 16\text{-}19}$ and $YopD_{\Delta 17\text{-}19}$. As a control, we used *Yersinia* producing $YopD_{\Delta 4\text{-}20}$, which has been described previously (57). All were examined for their ability to be produced and secreted by *Y. pseudotuberculosis.* As expected, secretion of $YopD_{\Delta 4\text{-}20}$ was virtually undetectable in our assay conditions (57), a phenotype now also shared by a new mutant producing $YopD_{\Delta 5\text{-}19}$ (Fig. 7A, lower panel). When quantified, levels of YopD variant secretion accounted for only 10.2% and 3.2% of the total protein produced respectively (Fig. 7B, light gray box). Moreover, deletions $YopD_{\Delta 6\text{-}19}$ (26.8%), $YopD_{\Delta 7\text{-}19}$ (49%), $YopD_{\Delta 8\text{-}19}$ (37.8%), $YopD_{\Delta 9\text{-}19}$ (27.9%) and $YopD_{\Delta 10\text{-}19}$ (54.5%) also displayed reduced secretion levels. However, progressively smaller deletions (such as $YopD_{\Delta 11\text{-}19}$, $YopD_{\Delta 12\text{-}19}$, $YopD_{\Delta 13\text{-}19}$, $YopD_{\Delta 14\text{-}19}$, $YopD_{\Delta 15\text{-}19}$, $YopD_{\Delta 16\text{-}19}$ and $YopD_{\Delta 17\text{-}19}$) as well as native YopD all maintained secretion competency (Fig. 7A, lower panel). For example, when expressed quantitatively this represented secretion levels in the order of 81.4% for $YopD_{\Delta 11\text{-}19}$ and 89.9% for native YopD (Fig. 7B, light gray box). As expected, secretion was totally absent from a control *Yersinia* strain lacking a functional T3SS (Δ*yscU,* Δ*lcrQ*) (Fig. 7A, lower panel). However, it was evident following quantification that the larger deletions all

tended to negatively impact on the amounts of Yops accumulated (Fig. 7B). This was observed for both YopD and YopE with accumulated intracellular pools only reaching between 36.3% to 70.4% of parent bacteria. At least for the YopD variants, we ruled out instability as a factor for this clear reduction in steady state levels, for native YopD and the deletion variants were equally resistant to endogenous proteases *in vivo* (Fig. 1). As lowered intracellular pools of protein would compromise secretion, we accounted for this by specifically quantifying the secretion efficiency of YopD and YopE from mutant bacteria compared to the parent. Notably, the secretion efficiency of all larger YopD deletion variants was still only a fraction of native YopD – within the range of 3.4% (for $YopD_{\Delta 5\text{-}19}$) and 60.5% ($YopD_{\Delta 10\text{-}19}$) (Fig. 7B, dark gray box). This contrasted with higher secretion efficiencies for the smaller deletion variants such as $YopD_{\Delta 11\text{-}19}$ (90.1%) (Fig. 7B, dark gray box and data not shown). Critically, the YopE secretion efficiency from all these mutant bacteria was also equivalent to parental bacteria (Fig. 7B, dark gray box). Thus, we can conclude that the $YopD_{\Delta 4\text{-}20}$, $YopD_{\Delta 5\text{-}19}$, $YopD_{\Delta 6\text{-}19}$, $YopD_{\Delta 7\text{-}19}$, $YopD_{\Delta 8\text{-}19}$, $YopD_{\Delta 9\text{-}19}$ and $YopD_{\Delta 10\text{-}19}$ variants all possess a bona fide secretion defect, in addition to and despite them having lower intracellular pools of accumulated protein.

To scrutinize if any particular codon or group of codons in this region are critically important for YopD secretion, extra sets of *in cis yopD* deletion mutations were created. We divided the analysis into three categories resulting in various combinations of in-frame deletions targeting a) residues 2 to 7 ($YopD_{\Delta 2\text{-}3}$, $YopD_{\Delta 2\text{-}4}$, $YopD_{\Delta 2\text{-}5}$, $YopD_{\Delta 3\text{-}4}$, $YopD_{\Delta 3\text{-}5}$, $YopD_{\Delta 3\text{-}6}$, $YopD_{\Delta 3\text{-}7}$, and $YopD_{\Delta 4\text{-}5}$) (Supplementary Fig. S3), b) residues 5 to 10 ($YopD_{\Delta 5\text{-}6}$, $YopD_{\Delta 5\text{-}7}$, $YopD_{\Delta 5\text{-}8}$, $YopD_{\Delta 5\text{-}9}$, $YopD_{\Delta 5\text{-}10}$, $YopD_{\Delta 6\text{-}10}$, $YopD_{\Delta 7\text{-}10}$, $YopD_{\Delta 8\text{-}10}$, and $YopD_{\Delta 8\text{-}10}$) (Supplementary Fig. S4), and c) all sequential residues through to position 19 ($YopD_{\Delta 2\text{-}3}$, $YopD_{\Delta 4\text{-}5}$, $YopD_{\Delta 6\text{-}7}$, $YopD_{\Delta 8\text{-}9}$, $YopD_{\Delta 10\text{-}11}$, $YopD_{\Delta 12\text{-}13}$, $YopD_{\Delta 14\text{-}15}$, $YopD_{\Delta 16\text{-}17}$, $YopD_{\Delta 18\text{-}19}$) (Supplementary Fig. S5). However, in no case did our analysis reveal any defect in YopD synthesis or secretion by *Y. pseudotuberculosis*. Hence, a systematic analysis of smaller deletions of the N-terminal region failed to pin-point any one codon, or group of codons, responsible for the YopD secretion defect observed in the larger deletions described in Fig. 7. It is also interesting that no smaller deletion lacking codon 3 and 5 were altered in YopD secretion, unlike our observations for $YopD_{I3,5N}$ (see Fig. 3). Currently, we have no definitive explanation for this disparity. Collectively, the vagaries of these results do suggest that no particular N-

terminal amino acid(s) need be essential for YopD secretion, so long as compensatory residues maintain the necessary physical characteristics of this N-terminal region.

Reduced YopD secretion impairs Yops translocation into eukaryotic cells. We now have multiple YopD variants with modifications of the N-terminus; only a few of these are defective in secretion. This permitted an opportunity to ascertain whether sequences within the YopD N-terminal secretor domain play any role in the ability of *Yersinia* to intoxicate target eukaryotic cells with Yop effector toxins. Thus, we performed a HeLa cell cytotoxicity assay that measures the effect of intracellularly localized YopE, a GTPase activating protein of the Rho family, on infected target cell morphology (62). As a control, we included the strain producing $YopD_{\Delta 4\text{-}20}$ that from an earlier study is known to be incapable of Yops translocation (57). We could only detect a similar impairment of the cytotoxicity response of eukaryotic cells when infected by *Yersinia* producing the poorly secreted YopD variants; bacteria producing $YopD_{low(x2)}$, $YopD_{\Delta 5\text{-}19}$ and $YopD_{\Delta 6\text{-}19}$ were non-cytotoxic, while the onset of cytotoxicity was quite delayed for the mutant producing $YopD_{Frame+1}$ (Fig. 8). All other YopD variants, including those with smaller N-terminal deletions, or even YopD with a dramatically altered N-terminal coding sequence, including $YopD_{Frame\text{-}1}$, $YopD_{high}$, $YopD_{low}$, and $YopD_{high(x2)}$ still maintained the capacity to efficiently intoxicate non-immune epithelial cells with the YopE cytotoxin (Fig. 8 and Supplementary Fig. S6). Our interpretation of this data is that the YopD N-terminus encompassing residues 2 to 20 appear to play no role in the translocation process *per se* other than to ensure that YopD is secreted.

The YopD N-terminus may assist with orchestrating secretion. We have previously shown that only minimal quantities of secreted native YopD is adequate for efficient Yops delivery into cells (19). Why then is *Y. pseudotuberculosis* that secretes low, but reproducibly detectable levels of YopD variants altered in their N-termini such a poor translocator of Yop effectors (see Fig. 8)? We considered that this chaperone-independent N-terminal secretion signal may contribute to temporal secretion control such that the timing of secretion of these modified YopD variants might be compromised. Since translocators are believed to function by forming pores in the eukaryotic cell plasma membrane through which effectors could possibly pass to gain access to the eukaryotic cell interior (53), failure to secrete them before the effectors could reduce translocation efficiency. We therefore examined if the N-terminus of secreted Yop substrates plays a part in orchestrating secretion. Chimeras were generated in which residues 2 to 15 of YopD were exchanged for the equivalent residues from YopE ($YopD_{E\text{-}Nterm}$) and vice versa ($YopE_{D\text{-}Nterm}$). Each chimeric allele was

introduced *in cis* onto the Ysc-Yop-encoding virulence plasmid to generate *Y. pseudotuberculosis* capable of producing either one or both of $YopD_{E\text{-}Nterm}$ and $YopE_{D\text{-}Nterm}$. No matter what the strain background, these chimeras were easily detected in association with bacteria and freely secreted into culture media (Fig. 9). As expected, a thorough quantification confirmed that these three chimeras were secreted with an efficiency equivalent to native protein (data not shown). Thus, under *in vitro* growth conditions of Ca^{2+} depletion in which T3S is considered to be at maximal activity, the YopD N-terminal secretion signal can be substituted with the equivalent region from an effector substrate without consequence. Moreover, the YopD N-terminus could also support secretion of the YopE substrate. At face value, this supports current dogma that conserved physical and/or chemical features of the N-terminus, rather than a consensus sequence of amino acids, determines a signal for T3S of all substrates.

However, *in vitro* induction of T3S is an all-or-nothing phenomenon that might not be synchronous due to various stages of T3SS assembly in a growing culture. This would negate any efforts to illustrate hierarchal secretion. Therefore, we turned to testing the temporal secretion of our chimeras in a bacterial viability assay associated with infections of macrophage-like J774-1 cell monolayers. This immune cell-based assay is far more stringent than the traditional epithelial cell-based YopE-dependent cytotoxic assay. In the latter, whether or not *Yersinia* can translocate YopE into HeLa cells has no consequence on bacterial survival. In contrast, the immune cell-based assay effectively distinguishes the functional status of T3SSs because T3S-defective *Yersinia,* or those devoid of one or more effectors, will be phagocytosed and destroyed by the anti-bacterial effects of an intracellular macrophage environment (7). In other words, these bacteria would be identifiable by reduced extracellular proliferation when associated with eukaryotic cells. Significantly, in such a cell based assay, only those T3SSs on the surface of bacteria in direct contact with eukaryotic cells are presumed to be functionally competent – thereby conferring synchronous effector translocation (63). Bacteria were incubated with cell monolayers for a sufficient time in order to attain target cell contact. Bacteria in suspension were removed and the proliferation of bacteria at the cell surface and after internalization was monitored over time by performing total viable counts. Data was expressed as a ratio of mutant to parental bacteria. The latter remains predominately extracellular and therefore ably proliferates during a 6 h incubation. Thus, a ratio below 1.0 implies that those mutant bacteria are less viable then the parent, whereas a ratio equivalent to 1.0 means that those mutant bacteria are as viable as the parent. As a positive control, we used bacteria producing $YopD_{high(x2)}$ that has a dramatically altered N-terminal

sequence that in no way effects the function of YopD. As expected, a ratio of ~1.0 at every time interval indicated that this mutant was as viable as parental bacteria (Fig. 10). This confirms our previous findings (see Fig. 8) that the YopD N-terminal sequence *per se* is not directly involved in the translocation process. As negative controls, we infected with bacteria lacking *yopD, yopE* or both. Progressively fewer bacteria were recovered as the experiment proceeded, such that at its conclusion (6h post-infection), around 5-fold less of these mutant bacteria were recovered compared to the parent (Fig. 10). Although not quite to the same extent, bacteria producing the $YopD_{E\text{-}Nterm}$ and/or $YopE_{D\text{-}Nterm}$ chimeras were also significantly less viable after 4 h and 6 h post-infection then *Yersinia* producing native YopD or $YopD_{high(x2)}$ (Mann-Whitney *U* test, $p < 0.05$) (Fig. 10). Hence, these chimeric bacterial strains were impaired in their ability to efficiently resist phagocytosis by the macrophage-like cells and were therefore subsequently exposed to various intracellular anti-bacterial killing strategies of the infected immune cells. Thus, these data might favor the existence of translocator- and effector-type N-terminal secretion signals that assist to establish appropriate temporal Yop secretion, which enables *Yersinia* to orchestrate Yop effector translocation to prevent bacterial uptake and avoid exposure to the anti-bacterial effects of an intracellular macrophage environment.

It is also possible that secretion signals have evolved specifically for and function best for only their cognate substrate. Thus, under stringent *in vivo* conditions any chimeric T3S substrate harboring a heterologous N-terminal secretion signal might by default be defective in delivery and/or function. To examine this, we constructed hybrid proteins with secretion signals from proteins of the same T3S substrate class. In particular, the N-terminal region of the YopB translocator was incorporated into YopD ($YopD_{B\text{-}Nterm}$) and the secretion signal of the YopH effector into YopE ($YopE_{H\text{-}Nterm}$). These two chimeras were also secreted with a relative efficiency similar to native protein (Fig. 9 and data not shown). We next performed a viability assay with bacteria producing these chimeric hybrids. Intriguingly, the viability of bacteria producing the $YopE_{H\text{-}Nterm}$ chimera over the entire 6 h infection period remained comparable to *Yersinia* producing native YopD or $YopD_{high(x2)}$ (Fig. 10). In contrast, *Yersinia* producing $YopD_{B\text{-}Nterm}$ survived poorly in our viability assay (Fig. 10). Hence, in the presence of host immune cells $YopE_{H\text{-}Nterm}$ with an alternate secretion signal from the same substrate class maintained proper secretion and function. Conversely, $YopD_{B\text{-}Nterm}$ with one other translocator secretion signal did not. Thus, it appears that Yop effector N-termini can be interchanged without any obvious detrimental effect so long as the swapped secretion signal sequence is derived from the same T3S substrate class (effector) and not from a different class (translocator). On the

other hand, YopD secretion and/or function is poorly preserved regardless of whether the exchanged sequence originated from an alternative translocator or from an effector. The native YopD N-terminus is therefore particularly critical for YopD function when the effectiveness of the Ysc-Yop T3SS is paramount (i.e.: in the presence of 'enemy' immune cells). In general terms therefore, our data support an earlier proposal (67) that translocators and effectors do have distinct chaperone-independent N-terminal secretion signals to assist in orchestrating temporal secretion.

Interestingly, when we used the standard HeLa cell cytotoxicity assay as a measure of YopE translocation, no difference in the translocation rate of native YopE or $YopE_{D\text{-}Nterm}$ produced by *Yersinia* containing either native YopD or $YopD_{E\text{-}Nterm}$ could be detected (Fig. 8 and Supplementary Fig. S6). As has already been suggested (12, 17, 19), the YopE-based cytotoxicity assay may not permit detection of subtle defects in Ysc-Yop T3SS functionality. Indeed, even some mutant bacteria capable of only modest YopD secretion ($YopD_{I3,5N}$, $YopD_{\Delta 7\text{-}19}$, $YopD_{\Delta 8\text{-}19}$, $YopD_{\Delta 9\text{-}19}$ and $YopD_{\Delta 10\text{-}19}$) were still fully cytotoxic to HeLa cell monolayers.

The first fifteen N-terminal residues act as an efficient T3S signal. Thus far, our analysis has indicated that the extreme YopD N-terminus contributes to secretion efficiency and may possibly influence temporal secretion control, although apparently not directly to effector translocation *per se*. To complete our study, we were curious as to whether these N-terminal residues could also function as an independent secretion signal to promote T3S of a signalless reporter, β-Lactamase. A series of translational fusions were generated between the 5′end of *yopD* (including the native SD sequence) and a signalless and promoterless *bla* allele. Plasmids were maintained *in trans* and expression of each fusion was controlled by an IPTG inducible promoter. For control purposes, we also generated a fusion in which the full-length *yopD* open reading frame was appended to promoterless *bla.* However, this generated a poorly expressed (Fig. 11A) and unstable (Supplementary Fig. S7) product that prevented meaningful comparisons to the shorter N-terminal fusions. Never the less, sequence of *yopD* encoding for the first 25, 20, 15 and 10 amino acids were all sufficient to produce generous levels of β-Lactamase, a portion of which was secreted. Secretion was readily observed by *Yersinia* lacking the native *yopB* and *yopD* alleles and also to a lesser extent by parental bacteria (Fig. 11A). This secretion was dependent on a functional T3SS because an isogenic *yopB, yopD* mutant also lacking an integral T3SS component, YscU, failed to secrete these fusions. Inhibited secretion by parental bacteria producing endogenous YopB and YopD is not surprising because one would expect native substrates to be

preferentially secreted – presumably mediated via the action of the cognate T3S chaperone LcrH – and this would then cause transient blockage of the T3SS channel. Critically, the secretion efficiency of $YopD_{10}$-Bla (16.4%) and $YopD_{15}$-Bla (79.7%) was less relative to $YopD_{20}$-Bla (Fig. 11B, dark gray box). Additionally, the $YopD_5$-Bla fusion was also secreted. However, this was only a fraction (1.3%) of $YopD_{20}$-Bla secretion (Fig. 11B, dark gray box), and was only visible in the translocator mutant background and often required over-exposure of the immunoblot (Fig. 11A). On the other hand, the smallest *yopD* fusions of 3 and 1 amino acids did not visibly promote secretion of the reporter, nor did a fusion containing the start codon together with 500 nt of upstream sequence (Fig. 11A). Hence, an efficient secretion signal of YopD is probably more than 10, but less than 16 N-terminal residues, whereas the first 5 amino acids may constitute the absolute minimal YopD secretion signal. Moreover, steady-state levels of accumulated $YopD_1$-Bla fusion was dramatically diminished being only 39.3% of synthesized $YopD_{20}$-Bla (Fig. 11B). This reduction could not be explained by a simple increase in protein turnover, for no difference in stability could be observed between any of these smaller fusions (Supplementary Fig. S7). This might suggest that the extreme YopD N-terminal sequence also contains an element(s) necessary for translation control. However, we acknowledge that other possibilities may also explain the low abundance of $YopD_1$-Bla in these steady-state experiments.

DISCUSSION

We investigated how the N-terminal secretion signal influences activity of the YopD translocator from the enteropathogenic *Y. pseudotuberculosis*. While we could not definitively rule out a mRNA-based secretion signal, experiments with frame-shifted mutants and the use of mRNA structural predictions indicate that the N-terminal secretion signal of YopD is more likely to be protein-based. In addition, codons for isoleucine at positions 3 and 5 were required for full YopD secretion. These two codons were a part of the absolute minimal secretion signal encompassing the first five residues of YopD. This signal enabled the signalless reporter protein β-Lactamase to be secreted via a T3S-dependent mechanism, although secretion levels increased appreciably with a larger YopD N-terminal sequence appended. These translational fusion studies also indicated that this extreme N-terminal sequence might contribute to the control of translation – a completely underappreciated feature of T3S control. Moreover, swapping the N-terminal secretion signal of YopD with the equivalent region derived from the translocated YopE effector or the YopB translocator

affected T3S function during *Yersinia*-immune cell contact, despite a normal Yop secretion profile *in vitro*. Collectively, these data not only identify the N-terminal sequence of YopD as a genuine secretion signal, but also as a possible mediator of translation control. Logically, these could be critical features necessary to coordinate the multiple activities of YopD, both in the bacterial cytoplasm and at the zone of contact between bacteria and the host cell.

By serendipity, we observed an apparent correlation between the length of the *yopD* 5′ coding sequence and the production level. This was most evident when examining the *yopD-bla* translation fusions; having only the *yopD*-derived AUG start codon dramatically reduced the level of β-Lactamase synthesis obtained. Efforts to further investigate this interesting phenotype were beyond the scope of this study. While we are still to rule out trivial differences in transcription levels or mRNA stability, at least we know that the low $YopD_1$-Bla yield is not due to an increase in protein turnover. Thus, it is tempting to speculate that a feature within the 5′ region of the *yopD* mRNA transcript might contribute to control of YopD translation. Several mechanisms of translation control are described in the literature and can involve both *cis*- and *trans*-acting factors, all of which are dependent upon the sequence and structure of the mRNA transcript (30, 42). If, as suspected, features of the 5′ end of the *yopD* mRNA transcript are important for translation control, a coupling between translation and secretion could be a theoretical possibility; an event likely to help prioritize YopD for secretion. Interestingly, translation and secretion coupling has already been proposed for substrates of the flagella-dependent T3SS (40).

The $YopD_{Frame+1}$ variant with an altered N-terminal protein sequence and only minor change to the mRNA sequence was poorly secreted. One might therefore consider the efficient secretion of the alternate frameshifted $YopD_{Frame-1}$ variant to be a contradiction. This frameshift mutation occurred after codon 4 to avoid introducing a premature stop codon. However, site-directed mutagenesis confirmed that retention of these native codons (encoding Thr_2 and Ile_3) were not the reason for efficient secretion. We believe that a more likely scenario is that the physical and/or chemical characteristics of N-terminal residues in $YopD_{Frame-1}$ fortuitously combine to enable its continued secretion. Of significance is the recent prediction that overall amphipathicity of the N-terminal secretion signal, with an enrichment of serine, threonine and proline, and possibly even short stretches of hydrophobic residues, are characteristics of a working T3S signal (6, 48, 64, 84). Interestingly, $YopD_{Frame-1}$ still harbors an N-terminus interspersed with hydrophobic residues and a relatively high proportion (5 of 15) of serine, threonine or proline residues; a pattern also observed for other

secretion competent YopD N-terminal sequences (see Table 2). In contrast, it is evident that the non-secreted $YopD_{Frame+1}$ secretion signal contains very few hydrophobic residues and also essentially lacks serine, threonine and proline residues (only 1 of 15). We therefore assume that these differences account for the secretion disparity among the two frameshifted mutants. This could also explain the slight reduction in $YopD_{I3,5N}$ secretion over $YopD_{Frame-1,\ I3,4N}$ secretion; while the proportions of serine, threonine or proline residues are consistent between the two, the former has a more restricted distribution of hydrophobic amino acids (see Table 2). It is also worth keeping in mind that N-terminal-mediated substrate secretion can be influenced by the sequence composition further downstream; T3S of YopR (also termed YscH) by *Yersinia* requires a distinct mRNA motif nearer to the C-terminus that cooperates with the typical N-terminal amino acid signal (9). The presence of such an internal secondary mRNA sequence has not been investigated for YopD.

In *Yersinia* evidence of a secretion hierarchy among T3S translocator and effector substrates is essentially absent in part due to inherent limitations of conventional *in vitro* assays. Ysc-Yop T3SS assembly would be asynchronous in a growing laboratory culture disguising any evidence of ordered secretion between early, middle and late substrates. Also masking orchestrated secretion *in vitro* is the low calcium response, an 'all-or-none phenomenon' that sees massive amounts of Yops synthesized and secreted when Ca^{2+} is specifically depleted (80). In contrast, bacteria in close association with target host cells are only thought to possess functional T3SSs at this contact zone (63). Therefore, hierarchal secretion is more likely to be observed during bacteria-host cell contact where only subsets of T3SSs are turned on simultaneously. In fact, real-time monitoring of this process has been reported for other bacteria (21, 51, 78, 82), but our laboratory is not yet equipped to perform such sophisticated experimentation. However, we did observe during infections of J774.1 macrophage-like cells that bacteria secreting YopD and YopE chimeras in which their respective N-terminal secretion signal domains were reciprocally exchanged were significantly more susceptible to host cell antibacterial killing than was parental *Yersinia*. These chimeras therefore sufficiently impair the T3S process such that bacteria are less able to use their T3SSs to promote survival when under siege from host cell innate immune defense mechanisms. This could imply that swapping the respective N-terminal secretion signals compromised temporal delivery of YopD and YopE.

If this hierarchal secretion model were true, why do the chimera producing strains all behave like the parental strain in the HeLa cell cytotoxicity assay? First of all, the cytotoxicity assay is not capable of

detecting subtle defects in Ysc-Yop T3SS functionality (12, 17, 19). Additionally, *Yersinia*-induced cytotoxicity and anti-phagocytosis are phenotypically unlinked; highly attenuated *yopE* point mutants are still cytotoxic towards HeLa cell monolayers, whereas bacteria defective in anti-phagocytosis are always avirulent (1, 75, 77). Accordingly, as an indirect measure of *Yersinia*-mediated anti-phagocytosis, we believe the viability assay to be a superior tool to ascertain T3SS function. In view of this, it might also be expected that bacteria co-producing $YopD_{E\text{-}Nterm}$ and $YopE_{D\text{-}Nterm}$ would show a more drastic reduction in viability (the timing being completely wrong as YopE would be secreted before YopD) in comparison with bacteria producing one or the other chimera (YopD and YopE would be secreted at the same time). However, one caveat of the viability readout is that it is not solely a measure of translocated YopE function. For example, *Yersinia* anti-phagocytosis also requires immediate delivery of the YopH phosphatase to the host cell interior (3, 5). It is likely that the influence of intracellular YopH activity could mask some of the subtle variances in viability of the three different YopD/YopE chimeric strains. It is also notable that T3S chaperones contribute to cognate substrate secretion (26). Since both $YopD_{E\text{-}Nterm}$ and $YopE_{D\text{-}Nterm}$ still maintain their cognate binding domains for the LcrH and SycE chaperones respectively (27, 83), a reasonable assumption is that native T3S chaperone piloting function is retained. Thus, this could also curb some of the effects of N-terminal domain swapping within the cognate substrates. With some justification therefore, we believe that our data is a reliable initial indicator that the N-terminal domain might be involved in orchestrating T3S, although definitive proof is still lacking.

So how might the chaperone-independent and chaperone-dependent secretion signals prioritize substrate secretion? Recent data indicates the existence of a large multiprotein cytoplasmic complex that could function as a T3S substrate sorting platform (44). Within this platform exists a conserved ATPase present in all T3SSs that is responsible for energizing substrate secretion (68, 70). Ample biochemical evidence indicates that effectors can interact with their cognate ATPase either directly or indirectly via their T3S chaperone (2, 10, 15, 33, 50, 68, 70, 73, 74). However, there is still no published report demonstrating binding between the ATPase and translocator-chaperone complexes. Moreover, tangible proof of the specificity underpinning the putative recognition mechanisms is thwarted by a scarcity of structural information on T3S ATPases either alone, or in association with T3S chaperone and/or substrate complexes (2, 37, 38, 86). It is therefore prudent to highlight alternative modes for substrate recognition and the creation of hierarchal secretion. In particular, translocator class T3S chaperones can selectively engage a membrane

associated T3SS component that exists in both flagella T3SSs (termed FliJ) (23) and non-flagella T3SSs (e.g.: InvI in *Salmonella* and YscO in *Yersinia*) (22). These protein complexes are thought to rapidly recycle empty translocator chaperones to collect new substrates to advance their secretion before late effector substrates. The InvE protein family present in a variety of T3SS-containing bacteria may also physically discriminate between middle and late substrate classes to prioritize translocator secretion (11, 18, 43, 49, 56, 85). In *Yersinia,* YopN and TyeA share homology with the N- and C-terminal regions of the InvE protein family, respectively. However, their loss does not specifically decrease YopB and YopD translocator secretion (25, 71), even though a YopD complex with TyeA has been reported (39). Finally, the integral inner membrane protein YscU – a core component of all T3SSs – might also distinguish between middle and late T3S substrates on the basis of differential recognition of the substrate N-terminus (61, 67), although this is not true for all homologues (8). We are currently endeavoring to unravel the relative contributions of all these parameters that may enable *Yersinia* to prioritize translocator secretion before secretion of the Yop effector arsenal begins.

At least for the Ysc-Yop T3SS, our data indicate that the N-terminus may contain structural information specific for translocator and effector substrate classes. This is not without precedent; in flagella T3SSs the molecular basis of early and late flagella substrate sorting is believed to involve such a structural demarcation (70). The fact that a YopE chimera containing the secretion signal of the YopH effector N-terminus did not compromise *Yersinia* T3S function supports this view. Yop effector substrates might contain a generic N-terminal sequence with shared characteristics that assist with ordering their secretion after the translocators. However, the situation appears far more complex for the multi-potent YopD protein on the basis that YopD chimeric function at the zone of bacteria-host cell contact was disrupted regardless of the exchanged N-terminal sequence being of translocator (YopB) or effector (YopE) origin. Whether this could be a universal phenomenon of all T3SSs remains unclear. The reciprocal exchange of N-terminal T3S secretion signals of enteropathogenic *Escherichia coli* (EPEC) translocator and effector proteins does not seem to interfere with function (54). While this might be at odds with our study, it is prudent to highlight that the EPEC study relies solely on *in trans* experimentation; all our chimeric constructs are stably placed *in cis* in the genome as a monocopy allele. There can be no doubting that this key difference would impact on phenotypic output making meaningful interpretation more difficult.

Given our evidence for the requirement of specific characteristics within individual N-terminal secretion signals for translocator and effector function, it is both impressive and curious that the artificial 'highx2' sequence functions normally for YopD (this study) and for YopE (47). It would be rewarding to understand what features of this synthetic sequence universally permits substrate secretion and function. However, these can only really be appreciated once the specific characteristics of each individual N-terminal secretion signal are unequivocally defined. We have used extensive molecular methods to reveal that YopD harbors an N-terminal secretion signal with peculiarities that make it distinct from other signals, but it has still proven impossible to pin-point what they actually are. Thus, now it is necessary to apply complementing biochemical and biophysical approaches in with the intention of making crucial advances in our knowledge of the T3S substrate secretion signal.

ACKNOWLEDGEMENTS

This work, performed within the framework of the Umeå Centre for Microbial Research (UCMR) Linnaeus Program (LP), was supported by grants from the Carl Tryggers Foundation for Scientific Research (MF), Swedish Research Council (ÅF, MF), Foundation for Medical Research at Umeå University (MF), Swedish Medical Association (MF) and J C Kempe Memorial Fund (AA).

We express gratitude to Hans Wolf-Watz for the gift of the parental *Yersinia* strain and various anti-Yop and anti-LcrV antibodies as well as to Andrew Roe for providing the plasmid pAJR104.

REFERENCES

1. **Aili, M., E. L. Isaksson, B. Hallberg, H. Wolf-Watz, and R. Rosqvist.** 2006. Functional analysis of the YopE GTPase-activating protein (GAP) activity of *Yersinia pseudotuberculosis*. Cell Microbiol **8:**1020-33.
2. **Akeda, Y., and J. E. Galan.** 2005. Chaperone release and unfolding of substrates in type III secretion. Nature **437:**911-5.
3. **Akopyan, K., T. Edgren, H. Wang-Edgren, R. Rosqvist, A. Fahlgren, H. Wolf-Watz, and M. Fallman.** 2011. Translocation of surface-localized effectors in type III secretion. Proc Natl Acad Sci U S A **108:**1639-44.
4. **Anderson, D. M., K. S. Ramamurthi, C. Tam, and O. Schneewind.** 2002. YopD and LcrH regulate expression of *Yersinia enterocolitica* YopQ by a posttranscriptional mechanism and bind to *yopQ* RNA. J Bacteriol **184:**1287-95.

5. **Andersson, K., K. E. Magnusson, M. Majeed, O. Stendahl, and M. Fallman.** 1999. *Yersinia pseudotuberculosis*-induced calcium signaling in neutrophils is blocked by the virulence effector YopH. Infect Immun **67:**2567-74.
6. **Arnold, R., S. Brandmaier, F. Kleine, P. Tischler, E. Heinz, S. Behrens, A. Niinikoski, H. W. Mewes, M. Horn, and T. Rattei.** 2009. Sequence-based prediction of type III secreted proteins. PLoS Pathog **5:**e1000376.
7. **Bartra, S., P. Cherepanov, A. Forsberg, and K. Schesser.** 2001. The *Yersinia* YopE and YopH type III effector proteins enhance bacterial proliferation following contact with eukaryotic cells. BMC Microbiol **1:**22.
8. **Bjornfot, A. C., M. Lavander, A. Forsberg, and H. Wolf-Watz.** 2009. Autoproteolysis of YscU of *Yersinia pseudotuberculosis* is important for regulation of expression and secretion of Yop proteins. J Bacteriol **191:**4259-67.
9. **Blaylock, B., J. A. Sorg, and O. Schneewind.** 2008. *Yersinia enterocolitica* type III secretion of YopR requires a structure in its mRNA. Mol Microbiol **70:**1210-22.
10. **Boonyom, R., M. H. Karavolos, D. M. Bulmer, and C. M. Khan.** 2010. *Salmonella* pathogenicity island 1 (SPI-1) type III secretion of SopD involves N- and C-terminal signals and direct binding to the InvC ATPase. Microbiology **156:**1805-14.
11. **Botteaux, A., M. P. Sory, L. Biskri, C. Parsot, and A. Allaoui.** 2009. MxiC is secreted by and controls the substrate specificity of the *Shigella flexneri* type III secretion apparatus. Mol Microbiol **71:**449-60.
12. **Broms, J. E., M. S. Francis, and A. Forsberg.** 2007. Diminished LcrV secretion attenuates *Yersinia pseudotuberculosis* virulence. J Bacteriol **189:**8417-29.
13. **Cambronne, E. D., and O. Schneewind.** 2002. *Yersinia enterocolitica* type III secretion: *yscM1* and *yscM2* regulate *yop* gene expression by a posttranscriptional mechanism that targets the 5' untranslated region of *yop* mRNA. J Bacteriol **184:**5880-93.
14. **Carlsson, K. E., J. Liu, P. J. Edqvist, and M. S. Francis.** 2007. Extracytoplasmic-stress-responsive pathways modulate type III secretion in *Yersinia pseudotuberculosis*. Infect Immun **75:**3913-24.
15. **Cooper, C. A., K. Zhang, S. N. Andres, Y. Fang, N. A. Kaniuk, M. Hannemann, J. H. Brumell, L. J. Foster, M. S. Junop, and B. K. Coombes.** 2010. Structural and biochemical characterization of SrcA, a multi-cargo type III secretion chaperone in *Salmonella* required for pathogenic association with a host. PLoS Pathog **6:**e1000751.
16. **Cornelis, G. R.** 2003. How Yops find their way out of *Yersinia*. Mol Microbiol **50:**1091-4.
17. **Costa, T. R., P. J. Edqvist, J. E. Broms, M. K. Ahlund, A. Forsberg, and M. S. Francis.** 2010. YopD self-assembly and binding to LcrV facilitate type III secretion activity by *Yersinia pseudotuberculosis*. J Biol Chem **285:**25269-84.
18. **Deng, W., Y. Li, P. R. Hardwidge, E. A. Frey, R. A. Pfuetzner, S. Lee, S. Gruenheid, N. C. Strynakda, J. L. Puente, and B. B. Finlay.** 2005. Regulation of type III secretion hierarchy of translocators and effectors in attaching and effacing bacterial pathogens. Infect Immun **73:**2135-46.
19. **Edqvist, P. J., M. Aili, J. Liu, and M. S. Francis.** 2007. Minimal YopB and YopD translocator secretion by *Yersinia* is sufficient for Yop-effector delivery into target cells. Microbes Infect **9:**224-33.
20. **Edqvist, P. J., J. E. Bröms, H. J. Betts, Å. Forsberg, M. J. Pallen, and M. S. Francis.** 2006. Tetratricopeptide repeats in the type-III-secretion chaperone, LcrH: their role in substrate binding and secretion. Mol Microbiol **59:**31-44.
21. **Enninga, J., J. Mounier, P. Sansonetti, and G. Tran Van Nhieu.** 2005. Secretion of type III effectors into host cells in real time. Nat Methods **2:**959-65.
22. **Evans, L. D., and C. Hughes.** 2009. Selective binding of virulence type III export chaperones by FliJ escort orthologues InvI and YscO. FEMS Microbiol Lett.
23. **Evans, L. D., G. P. Stafford, S. Ahmed, G. M. Fraser, and C. Hughes.** 2006. An escort mechanism for cycling of export chaperones during flagellum assembly. Proc Natl Acad Sci U S A **103:**17474-9.
24. **Feldman, M. F., S. Muller, E. Wuest, and G. R. Cornelis.** 2002. SycE allows secretion of YopE-DHFR hybrids by the *Yersinia enterocolitica* type III Ysc system. Mol Microbiol **46:**1183-97.
25. **Forsberg, Å., A. M. Viitanen, M. Skurnik, and H. Wolf-Watz.** 1991. The surface-located YopN protein is involved in calcium signal transduction in *Yersinia pseudotuberculosis*. Mol Microbiol **5:**977-86.
26. **Francis, M. S.** 2010. Type III secretion chaperones: a molecular toolkit for all occasions, p. 79-147. *In* P. Durante and L. Colucci (ed.), Handbook of molecular chaperones: roles, structures and mechanisms. Nova Science Publishers, Inc., Hauppauge, New York.

27. **Francis, M. S., M. Aili, M. L. Wiklund, and H. Wolf-Watz.** 2000. A study of the YopD-LcrH interaction from *Yersinia pseudotuberculosis* reveals a role for hydrophobic residues within the amphipathic domain of YopD. Mol Microbiol **38:**85-102.
28. **Francis, M. S., S. A. Lloyd, and H. Wolf-Watz.** 2001. The type III secretion chaperone LcrH co-operates with YopD to establish a negative, regulatory loop for control of Yop synthesis in *Yersinia pseudotuberculosis*. Mol Microbiol **42:**1075-93.
29. **Francis, M. S., and H. Wolf-Watz.** 1998. YopD of *Yersinia pseudotuberculosis* is translocated into the cytosol of HeLa epithelial cells: evidence of a structural domain necessary for translocation. Mol Microbiol **29:**799-813.
30. **Fredrick, K., and M. Ibba.** 2010. How the sequence of a gene can tune its translation. Cell **141:**227-9.
31. **Galan, J. E.** 2009. Common themes in the design and function of bacterial effectors. Cell Host Microbe **5:**571-9.
32. **Galan, J. E.** 2008. Energizing type III secretion machines: what is the fuel? Nat Struct Mol Biol **15:**127-8.
33. **Gauthier, A., and B. B. Finlay.** 2003. Translocated intimin receptor and its chaperone interact with ATPase of the type III secretion apparatus of enteropathogenic *Escherichia coli*. J Bacteriol **185:**6747-55.
34. **Goure, J., P. Broz, O. Attree, G. R. Cornelis, and I. Attree.** 2005. Protective anti-V antibodies inhibit *Pseudomonas* and *Yersinia* translocon assembly within host membranes. J Infect Dis **192:**218-25.
35. **Harrington, A. T., P. D. Hearn, W. L. Picking, J. R. Barker, A. Wessel, and W. D. Picking.** 2003. Structural characterization of the N terminus of IpaC from *Shigella flexneri*. Infect Immun **71:**1255-64.
36. **Hartland, E. L., S. P. Green, W. A. Phillips, and R. M. Robins-Browne.** 1994. Essential role of YopD in inhibition of the respiratory burst of macrophages by *Yersinia enterocolitica*. Infect Immun **62:**4445-53.
37. **Imada, K., T. Minamino, M. Kinoshita, Y. Furukawa, and K. Namba.** 2010. Structural insight into the regulatory mechanisms of interactions of the flagellar type III chaperone FliT with its binding partners. Proc Natl Acad Sci U S A **107:**8812-7.
38. **Imada, K., T. Minamino, A. Tahara, and K. Namba.** 2007. Structural similarity between the flagellar type III ATPase FliI and F1-ATPase subunits. Proc Natl Acad Sci U S A **104:**485-90.
39. **Iriarte, M., M. P. Sory, A. Boland, A. P. Boyd, S. D. Mills, I. Lambermont, and G. R. Cornelis.** 1998. TyeA, a protein involved in control of Yop release and in translocation of *Yersinia* Yop effectors. EMBO J **17:**1907-18.
40. **Karlinsey, J. E., J. Lonner, K. L. Brown, and K. T. Hughes.** 2000. Translation/secretion coupling by type III secretion systems. Cell **102:**487-97.
41. **Kim, B. H., H. G. Kim, J. S. Kim, J. I. Jang, and Y. K. Park.** 2007. Analysis of functional domains present in the N-terminus of the SipB protein. Microbiology **153:**2998-3008.
42. **Kozak, M.** 2005. Regulation of translation via mRNA structure in prokaryotes and eukaryotes. Gene **361:**13-37.
43. **Kubori, T., and J. E. Galán.** 2002. *Salmonella* type III secretion-associated protein InvE controls translocation of effector proteins into host cells. J Bacteriol **184:**4699-708.
44. **Lara-Tejero, M., J. Kato, S. Wagner, X. Liu, and J. E. Galan.** 2011. A sorting platform determines the order of protein secretion in bacterial type III systems. Science **331:**1188-9.
45. **Lavander, M., L. Sundberg, P. J. Edqvist, S. A. Lloyd, H. Wolf-Watz, and Å. Forsberg.** 2002. Proteolytic cleavage of the FlhB homologue YscU of *Yersinia pseudotuberculosis* is essential for bacterial survival but not for type III secretion. J Bacteriol **184:**4500-9.
46. **Lloyd, S. A., Å. Forsberg, H. Wolf-Watz, and M. S. Francis.** 2001. Targeting exported substrates to the *Yersinia* TTSS: different functions for different signals? Trends Microbiol **9:**367-71.
47. **Lloyd, S. A., M. Sjöström, S. Andersson, and H. Wolf-Watz.** 2002. Molecular characterization of type III secretion signals via analysis of synthetic N-terminal amino acid sequences. Mol Microbiol **43:**51-9.
48. **Löwer, M., and G. Schneider.** 2009. Prediction of type III secretion signals in genomes of gram-negative bacteria. PLoS One **4:**e5917.
49. **Martinez-Argudo, I., and A. J. Blocker.** 2011. The *Shigella* T3SS needle transmits a signal for MxiC release, which controls secretion of effectors. Mol Microbiol **78:**1365-78.
50. **Miki, T., Y. Shibagaki, H. Danbara, and N. Okada.** 2009. Functional characterization of SsaE, a novel chaperone protein of the type III secretion system encoded by *Salmonella* pathogenicity island 2. J Bacteriol **191:**6843-54.

51. **Mills, E., K. Baruch, X. Charpentier, S. Kobi, and I. Rosenshine.** 2008. Real-time analysis of effector translocation by the type III secretion system of enteropathogenic *Escherichia coli*. Cell Host Microbe **3:**104-13.
52. **Milton, D. L., R. O'Toole, P. Horstedt, and H. Wolf-Watz.** 1996. Flagellin A is essential for the virulence of Vibrio anguillarum. J Bacteriol **178:**1310-9.
53. **Mueller, C. A., P. Broz, and G. R. Cornelis.** 2008. The type III secretion system tip complex and translocon. Mol Microbiol **68:**1085-95.
54. **Munera, D., V. F. Crepin, O. Marches, and G. Frankel.** 2010. N-terminal type III secretion signal of enteropathogenic *Escherichia coli* translocator proteins. J Bacteriol **192:**3534-9.
55. **Neyt, C., and G. R. Cornelis.** 1999. Insertion of a Yop translocation pore into the macrophage plasma membrane by *Yersinia enterocolitica*: requirement for translocators YopB and YopD, but not LcrG. Mol Microbiol **33:**971-81.
56. **O'Connell, C. B., E. A. Creasey, S. Knutton, S. Elliott, L. J. Crowther, W. Luo, M. J. Albert, J. B. Kaper, G. Frankel, and M. S. Donnenberg.** 2004. SepL, a protein required for enteropathogenic *Escherichia coli* type III translocation, interacts with secretion component SepD. Mol Microbiol **52:**1613-25.
57. **Olsson, J., P. J. Edqvist, J. E. Bröms, Å. Forsberg, H. Wolf-Watz, and M. S. Francis.** 2004. The YopD translocator of *Yersinia pseudotuberculosis* is a multifunctional protein comprised of discrete domains. J Bacteriol **186:**4110-4123.
58. **Pallen, M. J., S. A. Beatson, and C. M. Bailey.** 2005. Bioinformatics, genomics and evolution of non-flagellar type-III secretion systems: a Darwinian perpective. FEMS Microbiol Rev **29:**201-29.
59. **Ramamurthi, K. S., and O. Schneewind.** 2005. A synonymous mutation in *Yersinia enterocolitica yopE* affects the function of the YopE type III secretion signal. J Bacteriol **187:**707-15.
60. **Ramamurthi, K. S., and O. Schneewind.** 2003. Yersinia *yopQ* mRNA encodes a bipartite type III secretion signal in the first 15 codons. Mol Microbiol **50:**1189-98.
61. **Riordan, K. E., and O. Schneewind.** 2008. YscU cleavage and the assembly of *Yersinia* type III secretion machine complexes. Mol Microbiol **68:**1485-501.
62. **Rosqvist, R., Å. Forsberg, and H. Wolf-Watz.** 1991. Intracellular targeting of the *Yersinia* YopE cytotoxin in mammalian cells induces actin microfilament disruption. Infect Immun **59:**4562-9.
63. **Rosqvist, R., K. E. Magnusson, and H. Wolf-Watz.** 1994. Target cell contact triggers expression and polarized transfer of *Yersinia* YopE cytotoxin into mammalian cells. EMBO J **13:**964-72.
64. **Samudrala, R., F. Heffron, and J. E. McDermott.** 2009. Accurate prediction of secreted substrates and identification of a conserved putative secretion signal for type III secretion systems. PLoS Pathog **5:**e1000375.
65. **Simon, R., U. Priefer, and A. Pühler.** 1983. A broad host range mobilisation system for in vivo genetic engineering: transposon mutagenesis in Gram negative bacteria. Biotechnology **1:**787-796.
66. **Skrzypek, E., and S. C. Straley.** 1995. Differential effects of deletions in *lcrV* on secretion of V antigen, regulation of the low-Ca2+ response, and virulence of *Yersinia pestis*. J Bacteriol **177:**2530-42.
67. **Sorg, I., S. Wagner, M. Amstutz, S. A. Muller, P. Broz, Y. Lussi, A. Engel, and G. R. Cornelis.** 2007. YscU recognizes translocators as export substrates of the *Yersinia* injectisome. EMBO J **26:**3015-24.
68. **Sorg, J. A., B. Blaylock, and O. Schneewind.** 2006. Secretion signal recognition by YscN, the *Yersinia* type III secretion ATPase. Proc Natl Acad Sci U S A **103:**16490-5.
69. **Sorg, J. A., N. C. Miller, and O. Schneewind.** 2005. Substrate recognition of type III secretion machines--testing the RNA signal hypothesis. Cell Microbiol **7:**1217-25.
70. **Stafford, G. P., L. D. Evans, R. Krumscheid, P. Dhillon, G. M. Fraser, and C. Hughes.** 2007. Sorting of early and late flagellar subunits after docking at the membrane ATPase of the type III export pathway. J Mol Biol **374:**877-82.
71. **Sundberg, L., and A. Forsberg.** 2003. TyeA of *Yersinia pseudotuberculosis* is involved in regulation of Yop expression and is required for polarized translocation of Yop effectors. Cell Microbiol **5:**187-202.
72. **Tardy, F., F. Homble, C. Neyt, R. Wattiez, G. R. Cornelis, J. M. Ruysschaert, and V. Cabiaux.** 1999. *Yersinia enterocolitica* type III secretion-translocation system: channel formation by secreted Yops. Embo J **18:**6793-9.
73. **Thomas, J., G. P. Stafford, and C. Hughes.** 2004. Docking of cytosolic chaperone-substrate complexes at the membrane ATPase during flagellar type III protein export. Proc Natl Acad Sci U S A **101:**3945-50.

74. **Thomas, N. A., W. Deng, J. L. Puente, E. A. Frey, C. K. Yip, N. C. Strynadka, and B. B. Finlay.** 2005. CesT is a multi-effector chaperone and recruitment factor required for the efficient type III secretion of both LEE- and non-LEE-encoded effectors of enteropathogenic *Escherichia coli*. Mol Microbiol **57:**1762-1779.
75. **Thorslund, S. E., T. Edgren, J. Pettersson, R. Nordfelth, M. E. Sellin, E. Ivanova, M. S. Francis, E. L. Isaksson, H. Wolf-Watz, and M. Fällman.** 2011. The RACK1 signaling scaffold protein selectively interacts with *Yersinia pseudotuberculosis* virulence function. PLoS ONE **6:**e16784.
76. **Troisfontaines, P., and G. R. Cornelis.** 2005. Type III secretion: more systems than you think. Physiology (Bethesda) **20:**326-39.
77. **Trulzsch, K., T. Sporleder, E. I. Igwe, H. Russmann, and J. Heesemann.** 2004. Contribution of the major secreted yops of *Yersinia enterocolitica* O:8 to pathogenicity in the mouse infection model. Infect Immun **72:**5227-34.
78. **Van Engelenburg, S. B., and A. E. Palmer.** 2008. Quantification of real-time *Salmonella* effector type III secretion kinetics reveals differential secretion rates for SopE2 and SptP. Chem Biol **15:**619-28.
79. **Wattiau, P., B. Bernier, P. Deslee, T. Michiels, and G. R. Cornelis.** 1994. Individual chaperones required for Yop secretion by *Yersinia*. Proc Natl Acad Sci U S A **91:**10493-7.
80. **Wiley, D. J., R. Rosqvist, and K. Schesser.** 2007. Induction of the *Yersinia* type 3 secretion system as an all-or-none phenomenon. J Mol Biol **373:**27-37.
81. **Williams, A. W., and S. C. Straley.** 1998. YopD of *Yersinia pestis* plays a role in negative regulation of the low-calcium response in addition to its role in translocation of Yops. J Bacteriol **180:**350-8.
82. **Winnen, B., M. C. Schlumberger, A. Sturm, K. Schupbach, S. Siebenmann, P. Jenny, and W. D. Hardt.** 2008. Hierarchical effector protein transport by the *Salmonella Typhimurium* SPI-1 type III secretion system. PLoS ONE **3:**e2178.
83. **Woestyn, S., M. P. Sory, A. Boland, O. Lequenne, and G. R. Cornelis.** 1996. The cytosolic SycE and SycH chaperones of *Yersinia* protect the region of YopE and YopH involved in translocation across eukaryotic cell membranes. Mol Microbiol **20:**1261-71.
84. **Yang, Y., J. Zhao, R. L. Morgan, W. Ma, and T. Jiang.** 2010. Computational prediction of type III secreted proteins from gram-negative bacteria. BMC Bioinformatics **11 Suppl 1:**S47.
85. **Yu, X. J., M. Liu, and D. W. Holden.** 2004. SsaM and SpiC interact and regulate secretion of *Salmonella* pathogenicity island 2 type III secretion system effectors and translocators. Mol Microbiol **54:**604-19.
86. **Zarivach, R., M. Vuckovic, W. Deng, B. B. Finlay, and N. C. Strynadka.** 2007. Structural analysis of a prototypical ATPase from the type III secretion system. Nat Struct Mol Biol **14:**131-7.
87. **Zuker, M.** 2003. Mfold web server for nucleic acid folding and hybridization prediction. Nucleic Acids Res **31:**3406-15.

1 TABLE 1. Bacterial strains used in this study

Strains	Genotype or phenotype	Source or reference
Strains		
Escherichia coli		
DH5	F$^-$, *recA*1, *endA*1, *hsdR*17, *supE*44, *thi*-1, *gyrA*96, *relA*1	Vicky Shingler
S17-1λpir	*recA*, *thi*, *pro*, *hsdR*$^-$*M*$^+$, Sm^R, <RP4:2-Tc:Mu:Ku:Tn7>Tp^R	(65)
TOP10	F$^-$, *mcrA*, Δ(*mrr-hsdRMS-mcrBC*), ϕ80*lacZ*ΔM15, Δ*lacX*74, *recA*1, *araD*139, (Δ*ara-leu*)7697, *galU*, *galK*, *rpsL* (Sm^R), *endA*1, *nupG*	Invitrogen
Yersinia pseudotuberculosis		
YPIII/pIB102	*yadA*::Tn5, Km^R (parent)	Hans Wolf-Watz
YPIII/pIB619	pIB102, *yopB* and *yopD* in-frame deletion, Km^R	(20)
YPIII/pIB619-75	pIB619, *yscU* in-frame deletion of codons 25 to 329, Km^R	This study
YPIII/pIB75	pIB102, *yscU* in-frame deletion, Km^R	(45)
YPIII/pIB75-26	pIB75, *lcrQ* in-frame deletion, Sp^R, Km^R	This study
YPIII/pIB522	pIB102, *yopE* in frame deletion, Km^R	(62)
YPIII/pIB522-625	pIB522, *yopD* in-frame deletion of codons 4 to 20, Km^r	(57)
YPIII/pIB625	pIB102, *yopD* in-frame deletion of codons 4 to 20, Km^R	(57)
YPIII/pIB577	pIB102, *yopE* harbouring the YopD secretion signal between codons 2 to 15, Km^R	This study
YPIII/pIB578	pIB102, *yopE* harbouring the YopH secretion signal between codons 2 to 15, Km^R	This study
YPIII/pIB62501	pIB625, *yopD* harbouring the YopE secretion signal between codons 2 to 15, Km^R	This study
YPIII/pIB62501-577	pIB62501, *yopE* harbouring the YopD secretion signal between codons 2 to 15, Km^R	This study
YPIII/pIB62502	pIB625, y*opD* with a +1 frame shift mutation after codon 1, Km^R	This study
YPIII/pIB62503	pIB625, y*opD* with a −1 frame shift mutation after codon 3, Km^R	This study
YPIII/pIB62304	pIB625, y*opD* with several wobble-base mutations between codons 2 to 16 altering only the mRNA sequence, Km^R	This study
YPIII/pIB62505	pIB625, y*opD* in frame deletion of codons 2 and 3, Km^R	This study
YPIII/pIB62506	pIB625, y*opD* in frame deletion of codons 4 and 5, Km^R	This study
YPIII/pIB62507	pIB625, y*opD* in frame deletion of codons 6 and 7, Km^R	This study
YPIII/pIB62508	pIB625, y*opD* in frame deletion of codons 8 and 9, Km^R	This study
YPIII/pIB62509	pIB625, y*opD* in frame deletion of codons 10 and 11, Km^R	This study
YPIII/pIB62510	pIB625, y*opD* in frame deletion of codons 12 and 13, Km^R	This study
YPIII/pIB62511	pIB625, y*opD* in frame deletion of codons 14 and 15, Km^R	This study
YPIII/pIB62512	pIB625, y*opD* in frame deletion of codons 16 and 17, Km^R	This study
YPIII/pIB62513	pIB625, y*opD* in frame deletion of codons 18 and 19, Km^R	This study
YPIII/pIB62514	pIB625, y*opD* with a synthetic hypothetical 7 codon high secretion signal, Km^R	This study
YPIII/pIB62537	pIB625, y*opD* with a synthetic hypothetical duplicated 7 codon high secretion signal, Km^R	This study

2

1

YPIII/pIB62515	pIB625, y*opD* with a synthetic hypothetical 7 codon low secretion signal, Km^R	This study
YPIII/pIB62538	pIB625, y*opD* with a synthetic hypothetical duplicated 7 codon low secretion signal, Km^R	This study
YPIII/pIB62524	pIB625, y*opD* in frame deletion of codons 5 to 19, Km^R	This study
YPIII/pIB62525	pIB625, y*opD* in frame deletion of codons 6 to 19, Km^R	This study
YPIII/pIB62526	pIB625, y*opD* in frame deletion of codons 7 to 19, Km^R	This study
YPIII/pIB62527	pIB625, y*opD* in frame deletion of codons 8 to 19, Km^R	This study
YPIII/pIB62528	pIB625, y*opD* in frame deletion of codons 9 to 19, Km^R	This study
YPIII/pIB62529	pIB625, y*opD* in frame deletion of codons 10 to 19, Km^R	This study
YPIII/pIB62530	pIB625, y*opD* in frame deletion of codons 11 to 19, Km^R	This study
YPIII/pIB62531	pIB625, y*opD* in frame deletion of codons 12 to 19, Km^R	This study
YPIII/pIB62532	pIB625, y*opD* in frame deletion of codons 13 to 19, Km^R	This study
YPIII/pIB62533	pIB625, y*opD* in frame deletion of codons 14 to 19, Km^R	This study
YPIII/pIB62534	pIB625, y*opD* in frame deletion of codons 15 to 19, Km^R	This study
YPIII/pIB62535	pIB625, y*opD* in frame deletion of codons 16 to 19, Km^R	This study
YPIII/pIB62536	pIB625, y*opD* in frame deletion of codons 17 to 19, Km^R	This study
YPIII/pIB62549	pIB625, y*opD* in frame deletion of codons 2 to 4, Km^R	This study
YPIII/pIB62550	pIB625, y*opD* in frame deletion of codons 2 to 5, Km^R	This study
YPIII/pIB62544	pIB625, y*opD* in frame deletion of codons 3 to 4, Km^R	This study
YPIII/pIB62555	pIB625, y*opD* in frame deletion of codons 3 to 5, Km^R	This study
YPIII/pIB62561	pIB625, y*opD* in frame deletion of codons 3 to 6, Km^R	This study
YPIII/pIB62556	pIB625, y*opD* in frame deletion of codons 3 to 7, Km^R	This study
YPIII/pIB62562	pIB625, y*opD* in frame deletion of codons 5 and 6, Km^R	This study
YPIII/pIB62551	pIB625, y*opD* in frame deletion of codons 5 to 7, Km^R	This study
YPIII/pIB62549	pIB625, y*opD* in frame deletion of codons 5 to 8, Km^R	This study
YPIII/pIB62563	pIB625, y*opD* in frame deletion of codons 5 to 9, Km^R	This study
YPIII/pIB62545	pIB625, y*opD* in frame deletion of codons 5 to 10, Km^R	This study
YPIII/pIB62560	pIB625, y*opD* in frame deletion of codons 6 to 10, Km^R	This study
YPIII/pIB62557	pIB625, y*opD* in frame deletion of codons 7 to 10, Km^R	This study
YPIII/pIB62565	pIB625, y*opD* in frame deletion of codons 8 to 10, Km^R	This study
YPIII/pIB62552	pIB625, y*opD* in frame deletion of codons 9 and 10, Km^R	This study
YPIII/pIB62546	pIB625, y*opD* encoding for the substitution of T_2G, Km^R	This study
YPIII/pIB62547	pIB62503, y*opD* with a −1 frame shift mutation after codon 3 and a substitution of T_2G, Km^R	This study
YPIII/pIB62539	pIB625, y*opD* encoding for the substitution of T_2N, Km^R	This study
YPIII/pIB62540	pIB62503, y*opD* with a −1 frame shift mutation after codon 3 and a substitution of T_2N, Km^R	This study
YPIII/pIB62554	pIB625, y*opD* encoding for the substitution of T_2K, Km^R	This study
YPIII/pIB62558	pIB62503, y*opD* with a −1 frame shift mutation after codon 3 and a substitution of T_2K, Km^R	This study
YPIII/pIB62541	pIB625, y*opD* encoding for the substitution of I_3G, Km^R	This study
YPIII/pIB62553	pIB62503, y*opD* with a −1 frame shift mutation after codon 3 and a substitution of I_3G, Km^R	This study
YPIII/pIB62548	pIB625, y*opD* encoding for the substitution of I_3N, Km^R	This study
YPIII/pIB62569	pIB62503, y*opD* with a −1 frame shift mutation after codon 3 and a substitution of I_3N, Km^R	This study
YPIII/pIB62542	pIB625, y*opD* encoding for the substitution of I_3K, Km^R	This study
YPIII/pIB62543	pIB62503, y*opD* with a −1 frame shift mutation after codon 3 and a substitution of I_3K, Km^R	This study
YPIII/pIB62559	pIB625, y*opD* encoding for the substitutions of I_3N and I_5N, Km^R	This study
YPIII/pIB62564	pIB62503, y*opD* with a −1 frame shift mutation after codon 3 and the substitutions of I_3N and I_4N, Km^R	This study

2

YPIII/pIB62577	pIB625, *yopD* harboring the YopB secretion signal between codons 2 to 15, Km^R	This study

TABLE 2. Comparison of the nucleotide and amino acid sequence changes in the YopD and YopE variants used in this study

Variant	Nucleotide and amino acid sequence encompassing codon positions 2 to 15																*In vitro* secretion competence
	1	2	3	4	5	6	7	8	9	10	11	12	13	14	15	16	
$YopD_{wt}$	atg M	aca T	ata I	aat N	atc I	aag K	aca T	gac D	agc S	cca P	att I	atc I	acg T	acc T	ggt G	tca S	Good
$YopD_{I3,5N}$	atg M	aca T	**aat N**	aat N	**aac N**	aag K	aca T	gac D	agc S	cca P	att I	atc I	acg T	acc T	ggt G	tca S	Reduced
$YopD_{Frame+1}$	atg M	aac N	aat N	aaa K	tat Y	caa Q	gac D	aga R	cag Q	ccc P	aat N	tat Y	cac H	gac D	cgg R	tca S	Poor
$YopD_{Frame-1}$	atg M	aca T	ata I	ata I	tca S	aga R	cag Q	aca T	gcc A	caa Q	tta L	tca S	cga R	ccg P	gtt V	tca S	Good
$YopD_{Frame-1, I3,4N}$	atg M	aca T	**aat N**	**aat N**	tca S	aga R	cag Q	aca T	gcc A	caa Q	tta L	tca S	cga R	ccg P	gtt V	tca S	Good
$YopD_{Scramble}$	atg M	acc T	att I	aac N	ata I	aaa K	act T	gat D	tct S	cct P	atc I	ata I	aca T	act T	ggc G	tca S	Good
$YopD_{high(x2)}$	atg M	ata I	att I	tct S	tca S	att I	agt S	agc S	ata I	att I	tct S	tca S	att I	agt S	agc S	tca S	Good
$YopD_{low(x2)}$	atg M	ata I	att I	att I	atc I	tct S	att I	ata I	ata I	att I	att I	atc I	tct S	att I	ata I	tca S	Poor*
$YopD_{high}$	atg M	ata I	att I	tct S	tca S	att I	agt S	agc S	agc S	cca P	att I	atc I	acg T	acc T	ggt G	tca S	Good
$YopD_{low}$	atg M	ata I	att I	att I	atc I	tct S	att I	ata I	agc S	cca P	att I	atc I	acg T	acc T	ggt G	tca S	Good
$YopE_{D-Nterm}$	atg M	aca T	ata I	aat N	atc I	aag K	aca T	gac D	agc S	cca P	att I	atc I	acg T	acc T	ggt G	tct S	Good
$YopD_{E-Nterm}$	atg M	aaa K	ata I	tca S	tca S	ttt F	att I	tct S	aca T	tca S	ctg L	ccc P	ctg L	acc P	aca T	tca S	Good
$YopE_{wt}$	atg M	aaa K	ata I	tca S	tca S	ttt F	att I	tct S	aca T	tca S	ctg L	ccc P	ctg L	acc P	aca T	tct S	Good

Shading in light grey indicates the $YopD_{wt}$ nucleotide triplets and their corresponding amino acid sequences. Dark grey shading indicates $YopE_{wt}$ sequence. Amino acid sequence boxed in a broken line is identical to wild type YopD, but the nucleotide sequence is altered ($YopD_{Scramble}$). Those regions unmarked possess different amino acid sequence while the nucleotide sequence is essentially the same ($YopD_{Frame+1}$ and $YopD_{Frame-1}$). The sequence shaded in light blue is artificial, and in another study (47) was seen to either promote (high) or abolish (low) YopE secretion. Boxes crossed with dark blue diagonal line highlight highly hydrophobic residues. Bold font indicates site-directed substitution mutations. The single asterisk indicates that synthesis of this variant was impaired.

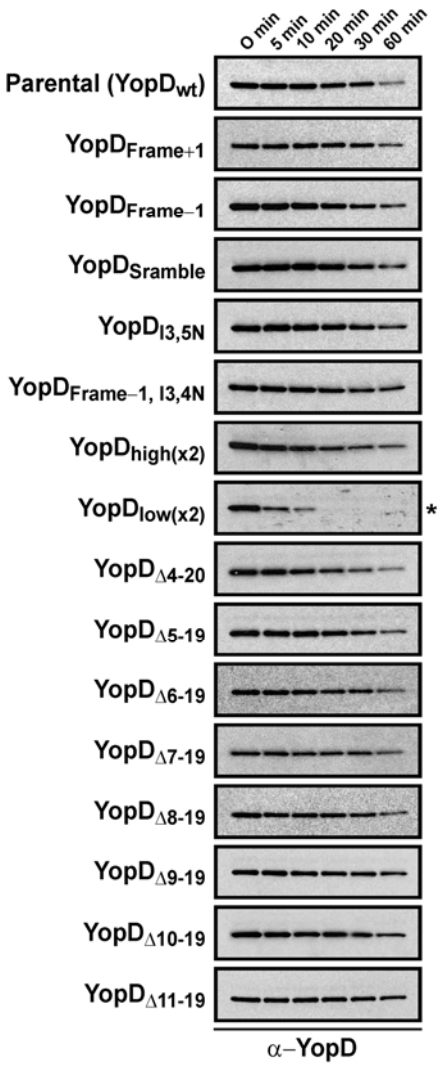

FIG. 1. Intrabacterial stability of pre-formed pools of various YopD mutant proteins. Bacteria were first cultured for 1 hour in non-inducing (plus 2.5 mM $CaCl_2$) BHI broth at 37°C. The protein synthesis inhibitor chloramphenicol (50 μg/ml) was added at time point 0 minutes (min). Samples were then collected at subsequent time points. Protein levels associated with pelleted bacteria were detected by Western blot using polyclonal anti-YopD antiserum. Panels: Parent (YopD$_{wt}$), YPIII/pIB102; YopD$_{Frame+1}$, YPIII/pIB62502; YopD$_{Frame-1}$, YPIII/pIB62503; YopD$_{Scramble}$, YPIII/pIB62504; YopD$_{I3,5N}$, YPIII/pIB62559; YopD$_{Frame-1, I3,4N}$, YPIII/pIB62564; YopD$_{high(x2)}$, YPIII/pIB62537; YopD$_{low(x2)}$, YPIII/pIB62538; YopD$_{\Delta 4-20}$, YPIII/pIB625; YopD$_{\Delta 5-19}$, YPIII/pIB62524; YopD$_{\Delta 6-19}$, YPIII/pIB62525; YopD$_{\Delta 7-19}$, YPIII/pIB62526; YopD$_{\Delta 8-19}$, YPIII/pIB62527; YopD$_{\Delta 9-19}$, YPIII/pIB62528; YopD$_{\Delta 10-19}$, YPIII/pIB62529; YopD$_{\Delta 11-19}$, YPIII/pIB62530. The asterisk (*) highlights YopD$_{low(x2)}$ as the only visibly unstable variant.

A

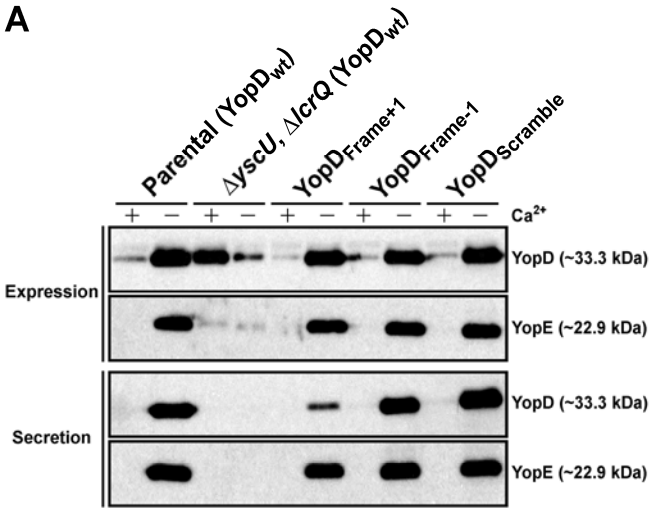

B

Strain	Percent total protein secreted		Percent of parent				Percent secretion efficiency$^{(y/x)}$	
			Total protein$^{(x)}$		Secreted protein$^{(y)}$			
	YopD	YopE	YopD	YopE	YopD	YopE	YopD	YopE
Parent	83.3 ± 7.4	73.1 ± 10.4						
$YopD_{Frame+1}$	25.2 ± 4.9	55.8 ± 17.6	92.9 ± 4.2	95.6 ± 4.9	27.0 ± 3.5	69.7 ± 12.7	29.3 ± 4.3$^{(**)}$	73.4 ± 13.5$^{(ns)}$
$YopD_{Frame-1}$	78.2 ± 8.3	75.2 ± 13.8	93.3 ± 2.5	92.4 ± 5.6	87.3 ± 5.3	94.0 ± 9.9	93.6 ± 5.6	100.9 ± 5.6
$YopD_{Scramble}$	90.0 ± 11.4	77.5 ± 15.7	95.3 ± 5.6	91.0 ± 3.8	102.0 ± 7.6	93.6 ± 5.8	109.0 ± 14.5	103.6 ± 8.4

FIG. 2. A YopD frameshift mutant altering the amino acid sequence of the N-terminal secretion signal specifically affects secretion. Overnight cultures were sub-cultured into BHI broth either containing (+) or lacking (–) calcium and then grown at 26°C for 1 h and then at 37°C for 3 hours. Protein samples were fractionated by a 12% SDS-PAGE and then transferred onto a membrane support for immune-detection (A). Expression fractions (upper panels) represent total protein associated with bacteria and also released into the culture supernatant. Secretion fractions (lower panels) signify protein freely released into the culture supernatant. Lanes: Parent ($YopD_{wt}$), YPIII/pIB102; Δ*yscU,* Δ*lcrQ* ($YopD_{wt}$), YPIII/pIB75-26; $YopD_{Frame+1}$, YPIII/pIB62502; $YopD_{Frame-1}$, YPIII/pIB62503; $YopD_{Scramble}$, YPIII/pIB62504. Molecular weights shown in parentheses are deduced from primary amino acid sequence. A minimum of three independent experiments was used to quantify relative YopD and YopE synthesis and secretion ± standard error of the mean using Quantity One software, version 4.52 (Bio-Rad) (B). "Percent total secretion" (lighter gray) reflects the ratio - expressed as a percentage - of protein secreted relative to the amount synthesized in each respective strain. "Percent secretion efficiency" reflects the extent of Yops secretion occurring in mutant bacteria relative to what occurs in parental bacteria (darker gray). It is calculated from the ratio of secreted protein relative to parent (^{y}) over total protein relative to parent (^{x}). Compared to native YopD, the median secretion efficiency of $YopD_{Frame+1}$ was significantly lower (**, p=0.079; non parametric Mann-Whitney U test, $p < 0.05$, two-tailed) then both $YopD_{Frame-1}$ and $YopD_{Scramble}$. In contrast, YopE secretion efficiency in these same strains was not statistically different from parent bacteria (*ns*, not significant; p=0.1143).

A

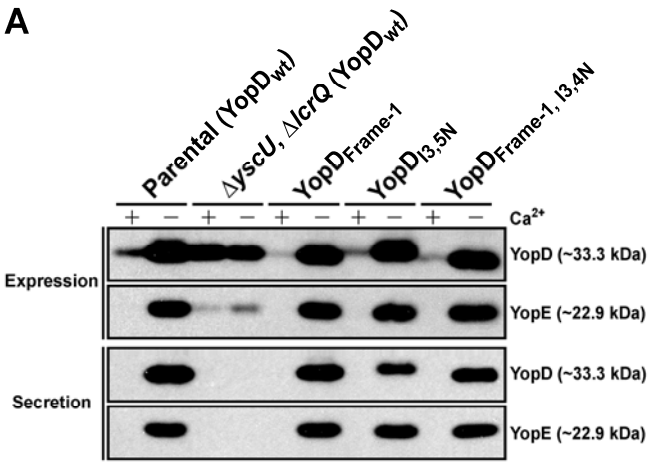

B

Strain	Percent total protein secreted		Percent of parent				Percent secretion efficiency$^{(y/x)}$	
			Total protein$^{(x)}$		Secreted protein$^{(y)}$			
	YopD	YopE	YopD	YopE	YopD	YopE	YopD	YopE
Parent	93.4 ± 4.6	80.5 ± 5.3						
$YopD_{Frame-1}$	92.5 ± 6.4	79.2 ± 6.7	93.6 ± 3.1	94.7 ± 5.3	92.7 ± 4.9	93.3 ± 7.0	98.8 ± 2.8	98.3 ± 1.9
$YopD_{I3,5N}$	51.4 ± 3.8	77.0 ± 2.8	96.4 ± 5.2	80.0 ± 14.7	52.7 ± 2.5	76.2 ± 11.9	55.5 ± 5.0$^{(*,**)}$	96.3 ± 3.3
$YopD_{Frame-1, I3,4N}$	75.6 ± 11.3	89.1 ± 8.4	88.8 ± 4.1	76.4 ± 22.2	71.0 ± 7.8	79.5 ± 12.8	79.8 ± 7.8$^{(ns)}$	113.0 ± 16.1

FIG. 3. N-terminal isoleucine residues contribute to secretion of native YopD. Overnight cultures were sub-cultured into BHI broth either containing (+) or lacking (–) calcium and then grown at 26°C for 1 h and then at 37°C for 3 hours. Protein samples were fractionated by a 12% SDS-PAGE and then transferred onto a membrane support for immune-detection (A). Expression fractions (upper panels) represent total protein associated with bacteria and also released into the culture supernatant. Secretion fractions (lower panels) signify protein freely released into the culture supernatant. Lanes: Parent ($YopD_{wt}$), YPIII/pIB102; Δ*yscU,* Δ*lcrQ* ($YopD_{wt}$), YPIII/pIB75-26; $YopD_{Frame-1}$, YPIII/pIB62503; $YopD_{I3,5N}$, YPIII/pIB62559 and $YopD_{Frame-1, I3,4N}$, YPIII/pIB62564;. Molecular weights shown in parentheses are deduced from primary amino acid sequence. The quantification of YopD and YopE secretion efficiency ± standard error of the mean was calculated from a minimum of three independent experiments using the Quantity One software, version 4.52 (Bio-Rad) (B). See the legend to Figure 2 for explanations of "Percent total secretion" (lighter gray) and "Percent secretion efficiency" (darker gray). Compared to native YopD, the median secretion efficiency of $YopD_{I3,5N}$ was significantly lower than $YopD_{Frame-1, I3,4N}$ (*, p=0.0317; non parametric Mann-Whitney *U* test, $p < 0.05$, two-tailed) or $YopD_{Frame-1}$ (**, p=0.079). Conversely, the observed secretion deficiency of $YopD_{Frame-1, I3,4N}$ was not considered to be statistically different from $YopD_{Frame-1}$ or native YopD (*ns*, not significant; p=0.1508).

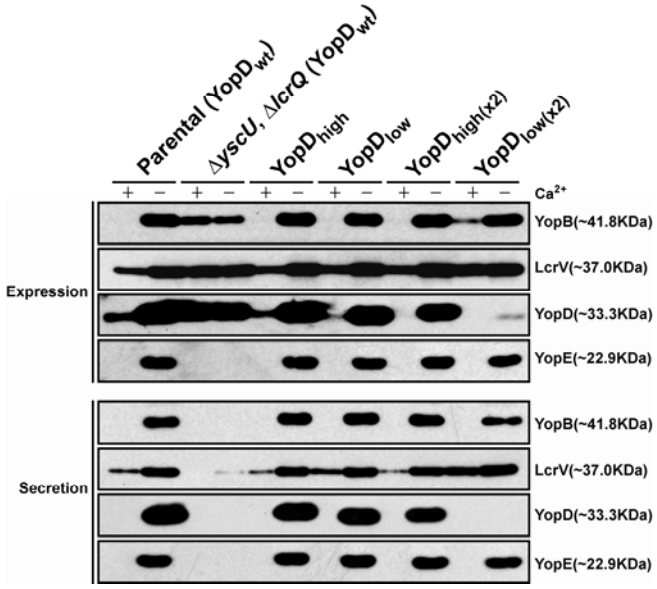

FIG. 4. Amphipathicity of the N-terminus is not an obvious mediator of YopD secretion. Overnight cultures were sub-cultured into BHI broth either containing (+) or lacking (–) calcium and then grown at 26°C for 1 h and then at 37°C for 3 hours. Protein samples were fractionated by a 12% SDS-PAGE and then transferred onto a membrane support for immune-detection. Expression fractions (upper panels) represent total protein associated with bacteria and also released into the culture supernatant. Secretion fractions (lower panels) signify protein freely released into the culture supernatant. Lanes: Parent ($YopD_{wt}$), YPIII/pIB102; Δ*yscU*, Δ*lcrQ* ($YopD_{wt}$), YPIII/pIB75-26; $YopD_{high}$, YPIII/pIB62514; $YopD_{low}$ YPIII/pIB62515; $YopD_{high(x2)}$, YPIII/pIB62537; and $YopD_{low(x2)}$, YPIII/pIB62538. Molecular weights shown in parentheses are deduced from primary amino acid sequence.

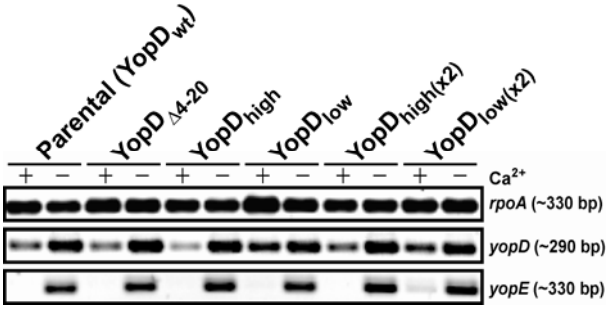

FIG. 5. RT-PCR of mRNA isolated from *Y. pseudotuberculosis*. RNA was isolated from log-phase bacterial cultures grown at 37°C in BHI medium with (+) and without (–) Ca^{2+}. Samples were subjected to RT-PCR using primers specific for *rpoA* (used as a loading control) and the T3SS genes *yopD* and *yopE*. Lanes: Parent ($YopD_{wt}$), YPIII/pIB102; $YopD_{\Delta 4\text{-}20}$, YPIII/pIB625; $YopD_{high}$, YPIII/pIB62514; $YopD_{low}$, YPIII/pIB62515; $YopD_{high(x2)}$, YPIII/pIB62537; $YopD_{low(x2)}$, YPIII/pIB62538. Images were acquired using a Fluor-S MultiImager (Bio-Rad). These were then inverted using the Quantity One quantitation software, version 4.52 (Bio-Rad). Numbers in parentheses indicated the approximate size of the amplified DNA fragment in base pairs (bp).

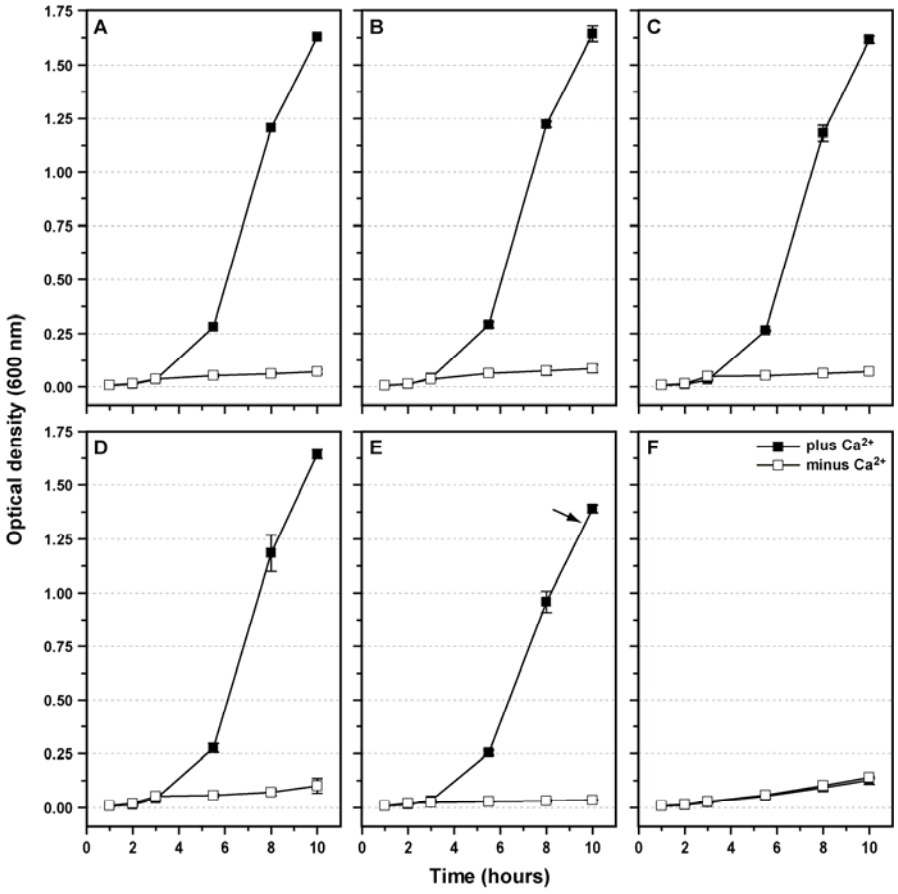

FIG. 6. Low calcium response growth phenotypes of *Y. pseudotuberculosis* producing various YopD variants. Bacteria were grown at 37°C in non-supplemented TMH medium (without Ca^{2+}; □) or supplemented with 2.5 mM $CaCl_2$ (with Ca^{2+}; ■). Three different growth phenotypes were detected: CD – calcium dependent growth (A to D); CD-like – moderate calcium dependent growth (E); TS – bacteria are sensitive to elevated temperature regardless of the presence of calcium (F). Panels: parental, YPIII/pIB102 (A); $YopD_{high}$, YPIII/pIB62514 (B); $YopD_{low}$ YPIII/pIB62515 (C); $YopD_{high(x2)}$, YPIII/pIB62537 (D); $YopD_{low(x2)}$, YPIII/pIB62538 (E); Δ*yscU,* Δ*lcrQ*, YPIII/pIB75-26 (F). The arrow highlights the subtle growth restriction of *Y. pseudotuberculosis* producing $YopD_{low(x2)}$.

A

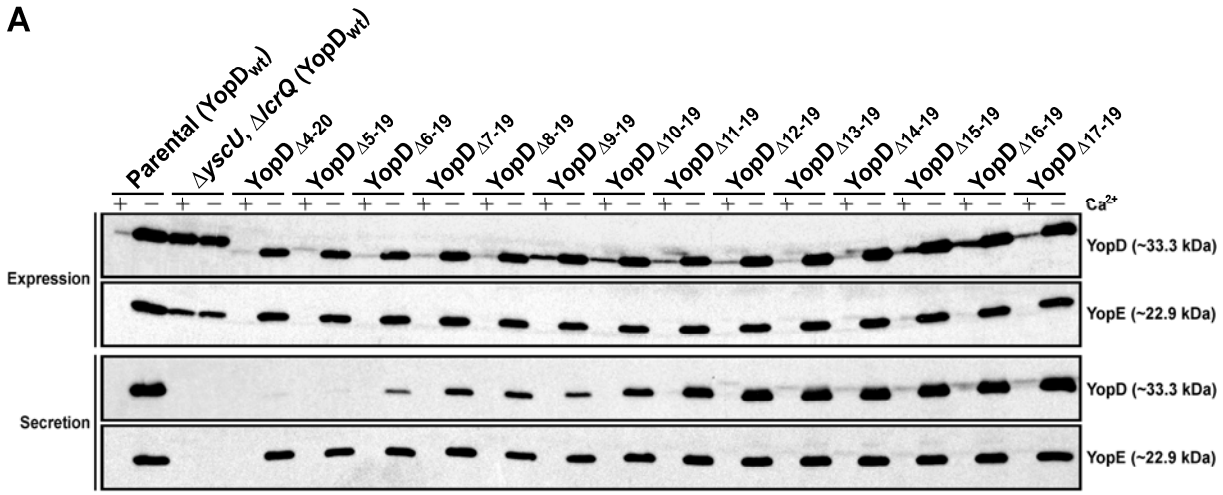

B

Strain	Percent total protein secreted		Percent of parent				Percent secretion efficiency$^{(y/x)}$	
			Total protein$^{(x)}$		Secreted protein$^{(y)}$			
	YopD	YopE	YopD	YopE	YopD	YopE	YopD	YopE
Parent	89.9 ± 6.1	74.4 ± 7.5						
YopD$_{Δ4-20}$	10.2 ± 1.3	91.1 ± 3.4	54.9 ± 1.9	58.5 ± 4.1	6.4 ± 1.2	72.1 ± 5.1	11.6 ± 2.3	124.4 ± 17.4
YopD$_{Δ5-19}$	3.2 ± 0.8	74.7 ± 13.7	53.7 ± 2.6	56.1 ± 2.5	1.9 ± 0.4	55.8 ± 2.2	3.4 ± 0.6	99.8 ± 8.4
YopD$_{Δ6-19}$	26.8 ± 0.6	71.1 ± 8.4	52.9 ± 5.7	64.4 ± 7.4	15.9 ± 2.3	61.3 ± 6.3	29.9 ± 1.5	95.3 ± 1.2
YopD$_{Δ7-19}$	49.0 ± 7.0	84.6 ± 0.4	56.5 ± 3.9	54.3 ± 7.3	30.7 ± 4.3	61.5 ± 2.3	53.9 ± 5.2	114.9 ± 11.2
YopD$_{Δ8-19}$	37.8 ± 9.5	86.8 ± 6.8	57.8 ± 4.0	50.1 ± 2.9	24.3 ± 6.1	58.5 ± 1.9	41.1 ± 8.6	116.9 ± 3.0
YopD$_{Δ9-19}$	27.9 ± 1.6	80.9 ± 22.2	60.6 ± 6.8	36.3 ± 9.8	13.1 ± 5.7	40.8 ± 17.5	19.9 ± 8.0	107.3 ± 19.3
YopD$_{Δ10-19}$	54.5 ± 3.7	74.1 ± 32.0	67.6 ± 4.5	43.8 ± 9.8	40.9 ± 3.0	45.6 ± 24.1	60.5 ± 1.7	94.0 ± 30.8
YopD$_{Δ11-19}$	81.4 ± 8.6	84.7 ± 20.3	70.4 ± 2.8	65.8 ± 6.4	63.2 ± 1.8	73.3 ± 3.5	90.1 ± 5.5	112.8 ± 16.2

FIG. 7. Expression and secretion of YopD containing various in-frame deletions of the N-terminal secretion signal. Overnight cultures were sub-cultured into BHI broth either containing (+) or lacking (–) calcium and then grown at 26°C for 1 h and then at 37°C for 3 hours. Protein samples were fractionated by a 12% SDS-PAGE and then transferred onto a membrane support for immune-detection (A). Expression fractions (upper panels) represent total protein associated with bacteria and also released into the culture supernatant. Secretion fractions (lower panels) signify protein freely released into the culture supernatant. Lanes: Parent (YopD$_{wt}$), YPIII/pIB102; Δ*yscU,* Δ*lcrQ* (YopD$_{wt}$), YPIII/pIB75-26; YopD$_{Δ4-20}$, YPIII/pIB625; YopD$_{Δ5-19}$, YPIII/pIB62524; YopD$_{Δ6-19}$, YPIII/pIB62525; YopD$_{Δ7-19}$, YPIII/pIB62526; YopD$_{Δ8-19}$, YPIII/pIB62527; YopD$_{Δ9-19}$, YPIII/pIB62528; YopD$_{Δ10-19}$, YPIII/pIB62529; YopD$_{Δ11-19}$, YPIII/pIB62530; YopD$_{Δ12-19}$, YPIII/pIB62531; YopD$_{Δ13-19}$, YPIII/pIB62532; YopD$_{Δ14-19}$, YPIII/pIB62533; YopD$_{Δ15-19}$, YPIII/pIB62534; YopD$_{Δ16-19}$, YPIII/pIB62535 and YopD$_{Δ17-19}$, YPIII/pIB62536. Molecular weights shown in parentheses are deduced from primary amino acid sequence. For a selection of mutants, YopD and YopE synthesis and secretion efficiency was quantified from at least three independent experiments using Quantity One software, version 4.52 (Bio-Rad) (B). Definitions of terms are provided in the legend to Figure 2.

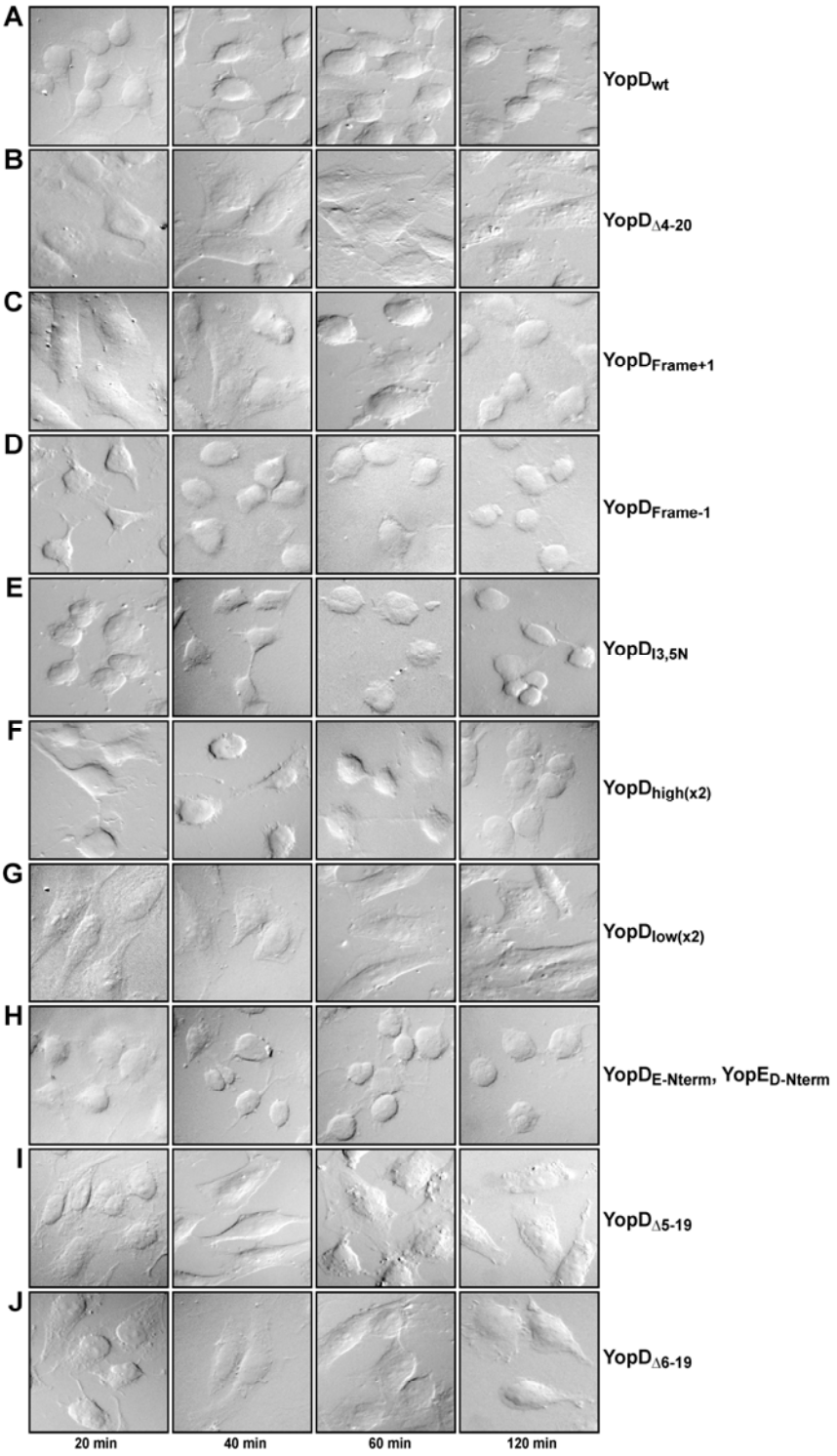

FIG. 8. Defects in YopD secretion impair Yops intoxication of infected eukaryotic cells. Strains were allowed to infect a monolayer of growing HeLa cells. At 20, 40, 60 and 120 minutes post infection, samples were fixated and the effect of the bacteria on the HeLa cells was recorded by phase-contrast microscopy. Translocation of the YopE cytotoxin, a GTPase-activating protein, causes a distinct rounding-up (cytotoxicity) of affected HeLa cells (see A, D, E and G). HeLa cells not intoxicated with YopE show normal uninfected cell morphology (see B, F and H). Some YopD variants reduced the efficiency of YopE translocation, which delayed the onset of cytotoxicity (see C and I). Panels: YopD$_{wt}$ (parent), YPIII/pIB102 (A); YopD$_{\Delta 4-20}$, YPIII/pIB625; (B); YopD$_{Frame+1}$, YPIII/pIB62502 (C); YopD$_{Frame-1}$, YPIII/pIB62503 (D); YopD$_{I3,5N}$, YPIII/pIB62559 (E); YopD$_{high(x2)}$, YPIII/pIB62537 (F); YopD$_{low(x2)}$, YPIII/pIB62538 (G); YopD$_{E-Nterm}$, YopE$_{D-Nterm}$, YPIII/pIB62501-577 (H); YopD$_{\Delta 5-19}$, YPIII/pIB62524 (I) and YopD$_{\Delta 6-19}$, YPIII/pIB62525 (J).

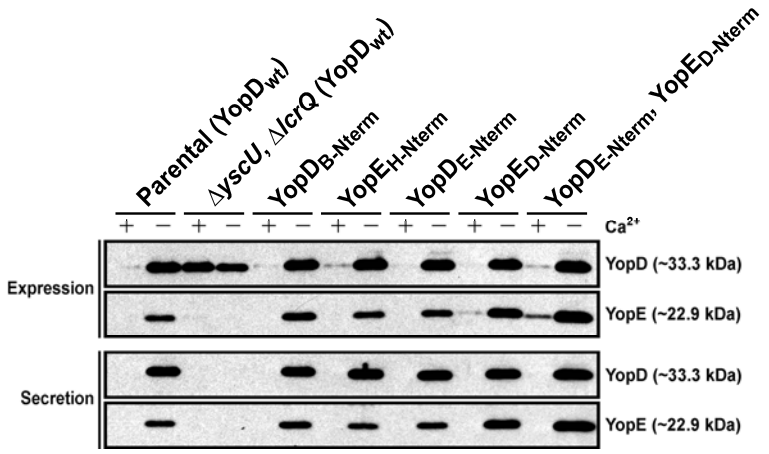

FIG. 9. Expression and secretion of YopD and YopE chimeras with a reciprocally exchanged N-terminal secretion signal. Overnight cultures were sub-cultured into BHI broth either containing (+) or lacking (–) calcium and then grown at 26°C for 1 h and then at 37°C for 3 hours. Protein samples were fractionated by a 12% SDS-PAGE and then transferred onto a membrane support for immune-detection. Expression fractions (upper panels) represent total protein associated with bacteria and also released into the culture supernatant. Secretion fractions (lower panels) signify protein freely released into the culture supernatant. Lanes: Parent ($YopD_{wt}$), YPIII/pIB102; Δ*yscU,* Δ*lcrQ* ($YopD_{wt}$), YPIII/pIB75-26; $YopD_{B\text{-}Nterm}$, YPIII/pIB62577; $YopE_{H\text{-}Nterm}$, YPIII/pIB578; $YopD_{E\text{-}Nterm}$, YPIII/pIB62501; $YopE_{D\text{-}Nterm}$, YPIII/pIB577; $YopD_{E\text{-}Nterm}$, $YopE_{D\text{-}Nterm}$, YPIII/pIB62501-577. Molecular weights shown in parentheses are deduced from primary amino acid sequence.

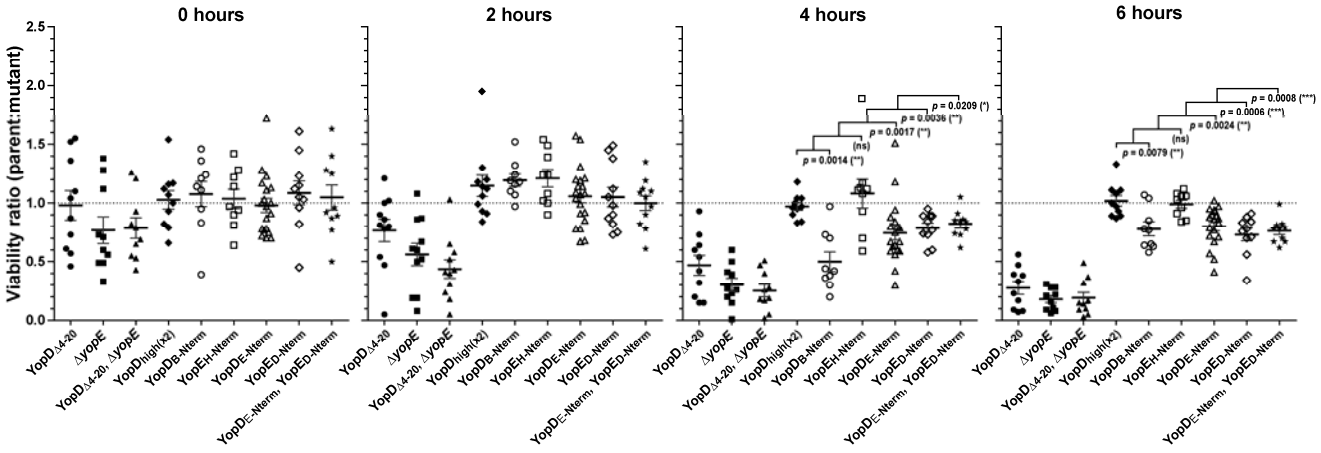

FIG. 10. Swapping Yop substrate N-terminal secretion signals compromise T3SS activity during contact with eukaryotic cells. *Yersinia* bacteria were used to infect monolayers of macrophage J774-1 cells (A). Those bacteria with a compromised T3SS are more rapidly phagocytosed and killed by the anti-bacterial activities of the cell. Bacterial viability was tested at the time of inoculation and thereafter 2 hr, 4 hr and 6 hr post-infection. The data is CFU/ml expressed as a ratio between mutant and parent bacteria. Each symbol indicates one independent experiment and the error bars represent ± standard error of the mean, which in turn is indicated as a short horizontal line. Bacteria producing one or both of $YopD_{E\text{-}Nterm}$ and $YopE_{D\text{-}Nterm}$ were always less viable suggesting a compromised order of YopD and YopE secretion. Bacteria either lacking YopE or failing to secrete YopD were even less viable. Strains: $YopD_{\Delta 4\text{-}20}$, YPIII/pIB625; Δ*yopE,* YPIII/pIB522; $YopD_{\Delta 4\text{-}20}$, Δ*yopE,* YPIII/pIB522-625; $YopD_{high(x2)}$, YPIII/pIB62537; $YopD_{B\text{-}Nterm}$, YPIII/pIB62577; $YopE_{H\text{-}Nterm}$, YPIII/pIB578; $YopD_{E\text{-}Nterm}$, YPIII/pIB62501; $YopE_{D\text{-}Nterm}$, YPIII/pIB577; $YopD_{E\text{-}Nterm}$, $YopE_{D\text{-}Nterm}$, YPIII/pIB62501-577. The asterisks (*, **, or ***) indicate that the chimeric variants are statistically less viable (Mann-Whitney *U* test, $p < 0.05$, two-tailed) than parent bacteria or bacteria producing $YopD_{high(x2)}$ after 4 h and 6 h incubation in the presence of J774-1 cell monolayers. On the other hand, the viability of bacteria producing $YopE_{H\text{-}Nterm}$ was comparable to these control bacteria (ns; not statistically significant).

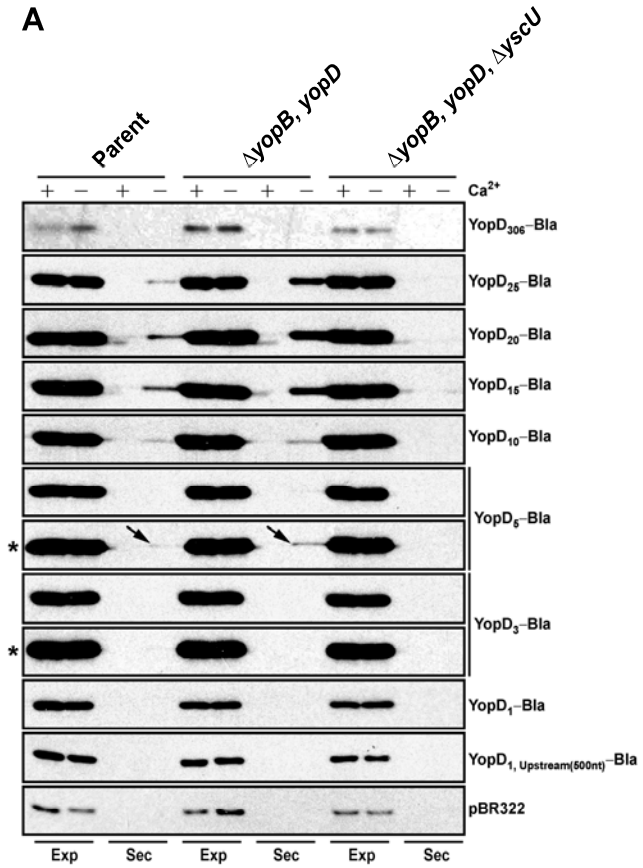

B

Construct (in Δ*yopB, yopD* background)	Percent total protein secreted	Percent of $YopD_{20}$-Bla		Percent secretion efficiency$^{(y/x)}$
		Total protein$^{(x)}$	Secreted protein$^{(y)}$	
$YopD_{20}$-Bla	86.1 ± 5.1			
$YopD_{15}$-Bla	44.8 ± 3.8	78.9 ± 3.0	62.6 ± 5.0	79.7 ± 7.1
$YopD_{10}$-Bla	9.9 ± 6.8	83.7 ± 4.1	14.3 ± 10.4	16.4 ± 11.2
$YopD_5$-Bla	0.8 ± 0.8	77.8 ± 2.3	1.1 ± 1.1	1.3 ± 1.3
$YopD_3$-Bla	nd	70.3 ± 2.5	nd	nd
$YopD_1$-Bla	nd	39.3 ± 3.3	nd	nd

FIG. 11. T3S of a β-lactamase reporter by appending the YopD N-terminus. Derivatives of pMMB208 contained *yopD::bla* translational fusions placed under control of an IPTG inducible promoter. These constructs were maintained in parental (YPIII/pIB102), Δ*yopB, yopD* (YPIII/pIB619) and Δ*yopB, yopD,* Δ*yscU* (YPIII/pIB619-75) bacteria. Overnight cultures of these bacteria were sub-cultured into BHI broth either containing (+) or lacking (–) calcium and then grown at 26°C for 1 h and then at 37°C for 3 hours. Expression fractions (Exp) representing total protein associated with bacteria and also released into the culture supernatant and secretion fractions (Sec) representing protein freely released into the culture supernatant, were fractionated by a 12% SDS-PAGE and then transferred onto a membrane support for immune-detection with rabbit polyclonal antisera recognizing β-lactamase (A). Panels: $YopD_{306}$–Bla, pAA113; $YopD_{25}$–Bla, pAA020, pAA020; $YopD_{20}$–Bla, pAA022; $YopD_{15}$–Bla, pAA025; $YopD_{10}$–Bla, pAA026; $YopD_5$–Bla, pAA027; $YopD_3$–Bla, pAA069; $YopD_1$–Bla, pAA028 and pBR322 (contains native β-lactamase). The asterisk highlights over-exposed panels. This enabled visualization of $YopD_5$::Bla fusion secretion (indicated by arrows), but not secretion of the $YopD_3$–Bla fusion; codons 1 to 5 may therefore represent the minimal N-terminal YopD secretion signal. The synthesis and secretion of selected fusions was quantified according to the legend to Figure 2. Limited by an acutely unstable full length $YopD_{306}$-Bla fusion, relative synthesis and secretion of the smaller truncated fusions was compared with $YopD_{20}$-Bla.